Research article

JGS
Journal of the Geological Society

https://doi.org/10.1144/jgs2022-130 | Vol. 180 | 2023 | jgs2022-130

Cambrian ages for metavolcanic rocks in the Lower Köli Nappes, Swedish Caledonides: implications for the status of the Virisen arc terrane

Isabel S. M. Carter[1,2*], Simon J. Cuthbert[1], Katarzyna Walczak[1], Grzegorz Ziemniak[3], Ellen Kooijman[4] and Jarosław Majka[1,2]

[1] Faculty of Geology, Geophysics and Environmental Protection, AGH University of Kraków, al. Mickiewicza 30, 30-059 Kraków, Poland
[2] Department of Earth Sciences, Uppsala University, Villavägen 16, SE-752 36 Uppsala, Sweden
[3] Institute of Geological Sciences, University of Wrocław, Pl. M. Borna 9, 50-204 Wrocław, Poland
[4] Department of Geosciences, Swedish Museum of Natural History, Stockholm, Sweden
ISMC, 0000-0001-7700-311X; SJC, 0000-0002-1029-6357; KW, 0000-0001-8944-1053; GZ, 0000-0003-3332-4725; EK, 0000-0003-2377-8272; JM, 0000-0002-6792-6866
* Correspondence: carter@agh.edu.pl

Abstract: The Köli Nappe Complex (KNC) of the Scandinavian Caledonide orogen originated as oceanic terranes within the Iapetus Ocean. These terranes have characteristics of magmatic arcs and associated forearc or back-arc basins and underwent several periods of rifting and magmatism prior to their accretion to the Baltican margin. We present new U–Pb zircon ages from the Lower Köli Ankarede Volcanite Formation in Västerbotten, Sweden. U–Pb ages of magmatic zircon grains from metamorphosed dacitic to andesitic rocks show ages of 512 ± 3.5, 497 ± 2, 491 ± 1 and 488 ± 4 Ma. The three younger ages fit with previous ages for Lower Köli volcanic rocks, but the 512 Ma age is older than any previous age for this unit. These dates constrain the age of magmatism in an ensimatic arc system within Iapetus. We compare this evolution with published information from the other Köli nappes. Magmatic ages within the KNC overlap with ages for an early episode of ultrahigh-pressure (UHP) metamorphism within the underlying Seve Nappe Complex (SNC), supporting the hypothesis that attributes UHP metamorphism within the SNC to subduction beneath the island arc now preserved within the Lower Köli Nappes.

Supplementary material: Photographs of sampled exposures (S1), BSE images of selected zircons (S2), charts of zircon trace elements (S3) and analyses of zircon (S4, S5) are available at https://doi.org/10.6084/m9.figshare.c.6843787

Thematic collection: This article is part of the Caledonian Wilson cycle collection available at: https://www.lyellcollection.org/topic/collections/the-caledonian-wilson-cycle

Received 30 August 2022; **revised** 18 August 2023; **accepted** 29 August 2023

Tectonostratigraphic terranes derived from the peripheral subduction systems within the Iapetus Ocean are a major feature of the orogenic architecture of the Scandinavian Caledonides, cropping out along much of the length (>1800 km) of this orogenic segment (Fig. 1). These lithotectonic assemblages offer a vast archive of information about the evolution of Iapetus and the development of accretionary orogens that predated the climactic Scandian collision of Baltica with Laurentia. These terranes also represent important examples of continental growth during the Phanerozoic by addition of island-arc magmatic edifices and their associated basin fills. The Iapetus terranes in Scandinavia form part of an even larger suite of Iapetus-derived terranes that extends through the British Isles and the North American segment of the Caledonian–Appalachian orogen (Fig. 1 inset).

In Scandinavia, the Iapetus terranes comprise a stack of thrusted allochthons, the largest of which comprise the Köli Nappe Complex (KNC) that outcrops in central and northern Sweden and the tectonostratigraphically equivalent Trondheim Nappe Complex (TNC) in central Norway (Fig. 1). Stephens and Gee (1985, 1989) erected a tectonostratigraphic terrane scheme for the Iapetus-derived magmatic-sedimentary assemblages in the Scandinavian Caledonides, in which the Lower Köli Nappes were equated with a 'Virisen terrane' (Stephens and Gee 1985; Stephens 2020) that they interpreted as the remnants of a rifted ensimatic arc located outboard of Baltica during the Late Cambrian and Early Ordovician. This postulated 'Virisen Arc' was then incorporated into an arc–continent collision model (Dallmeyer and Gee 1986) that attempted to explain a Late Cambrian eclogite-facies metamorphism (Stephens and van Roermund 1984; Andréasson *et al.* 1985; van Roermund 1985) in the underlying Seve Nappe Complex (SNC) (Fig. 1), thought to represent the subducted outer continental margin of Baltica (Gee 1975; Andréasson and Albrecht 1995).

Since these early studies, it has become clear that there has been widespread pre-Scandian high- to ultrahigh-pressure metamorphism in some elements of the SNC (e.g. Brueckner and van Roermund 2007; Root and Corfu 2012; Klonowska *et al.* 2017; Bukała *et al.* 2018; Barnes *et al.* 2019, 2020; Walczak *et al.* 2022*b*). This suggests that there was at least one major continental subduction episode along the Iapetan periphery of Baltica and poses questions about the identity of the terrane (or terranes) that Baltica collided with. The Virisen Arc was postulated in the 'dunk tectonics' models of Brueckner and van Roermund (2004) and Brueckner (2006) that attempted to explain multiple subductions of the Baltica margin during the Caledonian orogenic cycle. Here, collision with this postulated arc terrane explained the earliest eclogite facies metamorphism in the SNC. Subsequent closure of the intervening seaway was proposed to have resulted in a second eclogite-facies metamorphism in the main continental margin of

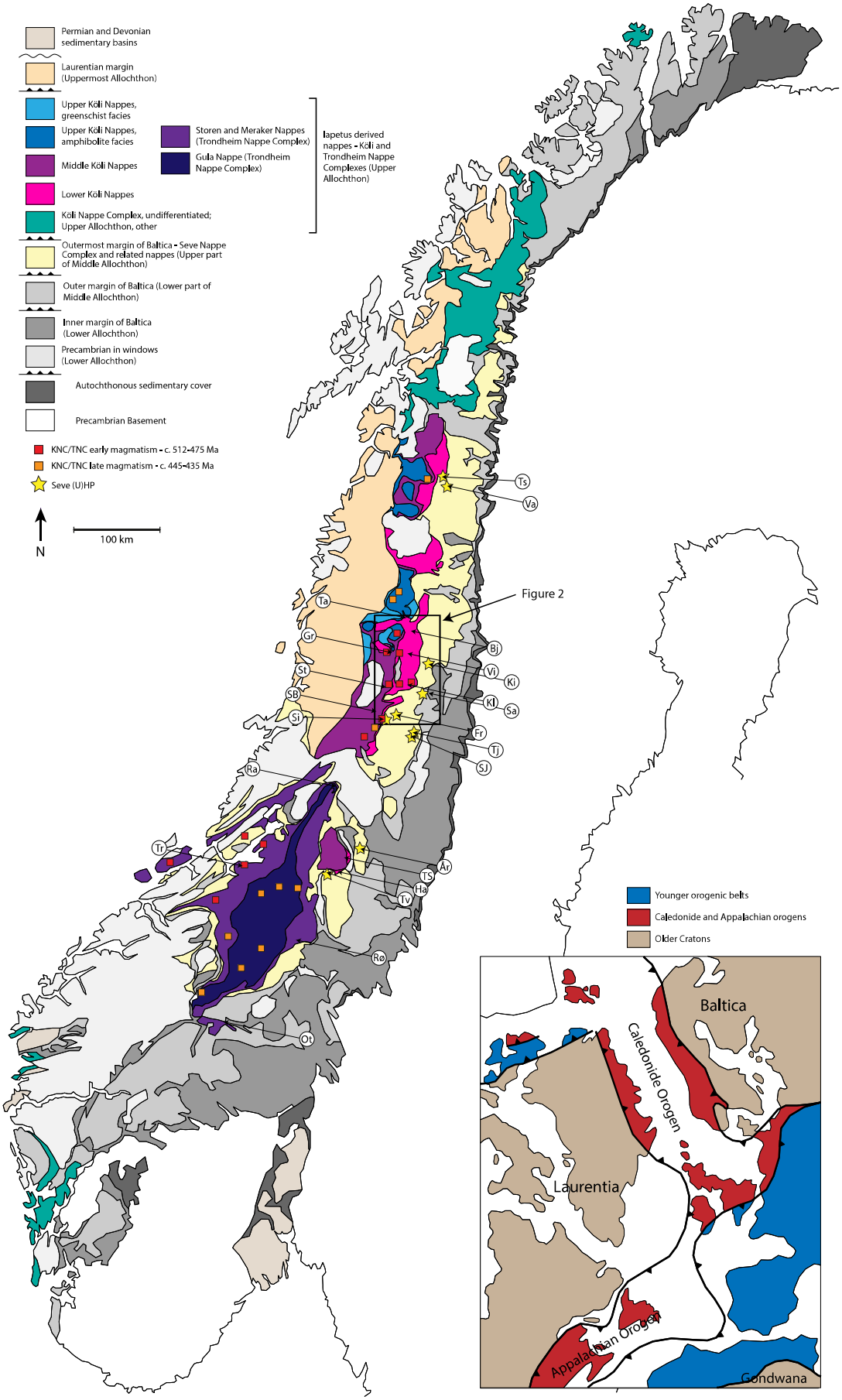

Fig. 1. Tectonostratigraphic map of the Scandinavian Caledonides, showing locations of dated occurrences of magmatism within the Köli Nappe Complex (KNC) and Trondheim Nappe Complex (TNC), and of ultrahigh-pressure (UHP) metamorphism within the Seve Nappe Complex. Abbreviations (from bottom to top): Ot, Otta (Gudbrandsdal); Rø, Røros; Tr, Trondheim; Tv, Tvarnklumparna; Ha, Handöl; TS, Tannförsen Synform; År, Åreskutan; Ra, Raudfjellet; SJ, Stor Jougdan; Tj, Tjeliken; Si, Sipmikk; SB, Störa Blåsjön; Fr, Frinningen; St, Stekenjokk; Sa, Saxnas; Kl, Klimpfjall; Ki, Kittelfjall; Vi, Virisen; Gr, Gränsjö; Bj, Björkvattnet; Ta, Tärnaby; Va, Vaimok; Ts, Tsäkkok. Inset map shows palaeogeography of the North Atlantic Caledonides in the Mesozoic. Source: modified after Gee *et al.* (1985); inset modified after Gee and Stephens (2020).

Baltica in the Middle to Late Ordovician, now preserved within the SNC in Jämtland. A similar model of arc collision, while not explicitly naming the Virisen terrane, was proposed by Majka *et al.* (2014*a*).

The success of such arc-collision models depends upon knowledge of the linkages between the KNC and SNC and their chronology. However, the juxtaposition of these terranes remains to be well documented both in terms of structural-metamorphic evolution or detailed timing. Furthermore, the detailed origins of the Virisen terrane arc and back-arc rocks are not well understood; there are few data on the provenance of the basin-fill metasedimentary rocks (Gee *et al.* 2014) and the timing of arc and arc-rifting magmatism (Claesson *et al.* 1983), and there has been limited further research on the nature and sources of magmatism since the early work in the 1970s and 1980s (summarized by Stephens *et al.* 1985*a*; Stephens 2020). In this contribution, we present new zircon U–Pb ages for felsic volcanic or subvolcanic rocks of the Lower Köli Nappes in the Virisen terrane type area. We find that a previous multi-grain zircon U–Pb age in the Late Cambrian to Early Ordovician (Claesson *et al.* 1983) is confirmed, but the range of our new ages extends into the Early Cambrian, which is considerably older than any known Iapetus intra-oceanic magmatism and has important implications for the timing of subduction initiation in Iapetus.

Palaeogeographical context

The Iapetus Ocean resulted from the rifting and break-up of the Rodinia supercontinent in the Neoproterozoic (or possibly Early Cambrian), creating the palaeo-continents of Laurentia, Gondwana and Baltica (Pickering and Smith 1995; Cawood *et al.* 2016; Robert *et al.* 2021). Between ~700 and 565 Ma a number of continental ribbon terranes rifted from Laurentia, Gondwana and Baltica (Roberts *et al.* 2007; Domeier 2016; Robert *et al.* 2021). These continental terranes were dispersed within Iapetus alongside younger arc terranes and all subsequently became incorporated into the Caledonide allochthons; some may have formed the foundations for intra-oceanic arcs (e.g. Hollocher *et al.* 2012). Subduction was active in Iapetus from the latest Cambrian (Torsvik and Cocks 2013; Domeier 2016). Evidence for subduction and the development of magmatic arcs along the eastern margin of Laurentia (modern geographical framework) and its continuation through the British Isles are well established (see Chew and Strachan 2014; Van Staal and Dewey 2023; Van Staal and Zagorevski 2023). Subduction directly outboard of Baltica is a more controversial topic, and faunas outside the area where Laurentian links are clear are sparse and often poorly preserved (Bruton and Harper 1988) or indicate mid-Iapetan rather than Baltican provincialism. However, some mechanism is required to explain (ultra-)high-pressure metamorphism in the underlying SNC at a time when most palaeogeographical reconstructions show Iapetus as a wide ocean basin, and so without a continent opposing Baltica (Domeier 2016; Cocks and Torsvik 2021). Cocks and Torsvik (2005) proposed a subduction zone along the Baltican margin of the Aegir Ocean opposite Siberia during the Late Cambrian and, subsequently (based on more tenuous evidence), along the Iapetus seaboard in the Early Ordovician following Baltica's rotation to face Laurentia. Final closure of Iapetus initiated by 440–430 Ma due to the collision of Baltica with Laurentia, although at this early stage localized extension and associated magmatism continued as collision proceeded in other segments (Slagstad and Kirkland 2018; Stephens 2020; Jakob *et al.* 2022). Continuing collision ultimately led to the emplacement of the allochthons on to Baltica and subduction of the western edge of the Baltica basement (forming the Western Gneiss Region (U)HP terrane) in the Scandian orogeny ~430–400 Ma (Chew and Strachan 2014; Corfu *et al.* 2014). (Hacker *et al.* 2010).

Tectonostratigraphy of the Köli Nappe Complex

Overview

The KNC generally comprises metavolcanic and metasedimentary rocks of mainly Cambrian and Ordovician age, and commonly of oceanic character. Magmatic rocks often have recognizable affinities to island-arc systems and sedimentary rocks comprise large accumulations of greywackes with pelagic mud-rocks (flysch) probably formed in subduction-related marginal basins. Latest Ordovician or earliest Silurian plutonic complexes are associated with lithospheric extension. Internally, the KNC is a stack of nappes, often discontinuous along-strike. Major tectonic discontinuities and differences between their internal stratigraphic sequences allow three nappe sequences to be defined – the Lower, Middle and Upper Köli Nappes (Stephens 1980, 2020).

Lower Köli Nappes

In north Jämtland and Västerbotten, the Lower Köli Nappes (LKN) mainly comprise the Björkvattnet Nappe (Kulling 1933; Stephens 1977; Greiling and Grimmer 2007). Its equivalent, extending west of Tärnaby towards Hattfjelldal in Norway, is the similar Joesjö Nappe (Häggbom 1978), although this was placed in the Middle Köli Nappes (MKN) by Saalmann *et al.* (2021). The outcrop of the Björkvattnet Nappe is defined by two major north–south-trending D_3 synforms on either side of the basement-cored Fjällfjäll antiform (Fig. 2). In the eastern limb of the Eastern Synform (Virisen–Björkvattnet–Tärnaby area, Fig. 3), the lowest strata are metabasalts with subordinate phyllite and local conglomerate of the Seima Formation (Stephens *et al.* 1985*b*), equivalent to the Kvemoen Mica Schist and Hapkebakte Conglomerate in the more southerly Klimpfjäll area towards the southern terminus of the Eastern Synform (Sjöstrand 1978; Greiling and Grimmer 2007). These are succeeded by the flysch-like Gilliks Formation comprising quartz-rich, turbiditic sandstones, phyllites and conglomerates with granitoid, carbonate, mafic and ultramafic clast assemblages. There are also horizons of felsic and mafic tuff (Stephens *et al.* 1985*b*). In the Western Synform and towards the southern terminus of the Eastern Synform (Gränssjö and Klimpfjäll areas, Fig. 3), the lower part of the Björkvattnet Nappe was not differentiated in the early surveys and all strata older than Late Ordovician were allocated to the Tjopasi Group (Zachrisson 1969), encompassing equivalents of the Seima and Gilliks formations.

The Seima and Gilliks formations and the lower part of the Tjopasi Group contain numerous lensoid, solitary serpentinites (DuRietz 1935). They lie within phyllite, mica schist and metabasalt in the Seima Formation and equivalents (termed the Rotik or Ro Conglomerate 'series' by Kulling (1933)). They commonly have a monomict detrital serpentinite conglomerate carapace and lie upon quartzite conglomerate (also monomict), having invasive relationships (Zachrisson 1969) that suggest the serpentinite was, at least partially, in a fluid state when emplaced. Grimmer and Greiling (2012) found them to have compositions similar to depleted mantle peridotites but with anomalously high Sb, As and Pb indicating fluxing by subduction fluids; they proposed an origin as serpentine mud volcanoes in a forearc basin.

In major 'cross-folds' around Klimpfjäll (south) and Skalmodal (north) in the Western Synform and towards the southern terminus of the Eastern Synform (Figs 2, 3), the Tjopasi Group includes the Ankarede Volcanite Formation (AVF), consisting of both acid and intermediate metavolcanic rocks with subordinate metabasalts, the latter having trace element patterns typical of island-arc tholeiites (Grimmer and Greiling 2012). The continuous range of compositions from basalt through andesite to dacite also supports a magmatic arc origin. It was this unit that was sampled for the study presented in this paper. The unit has undergone significant

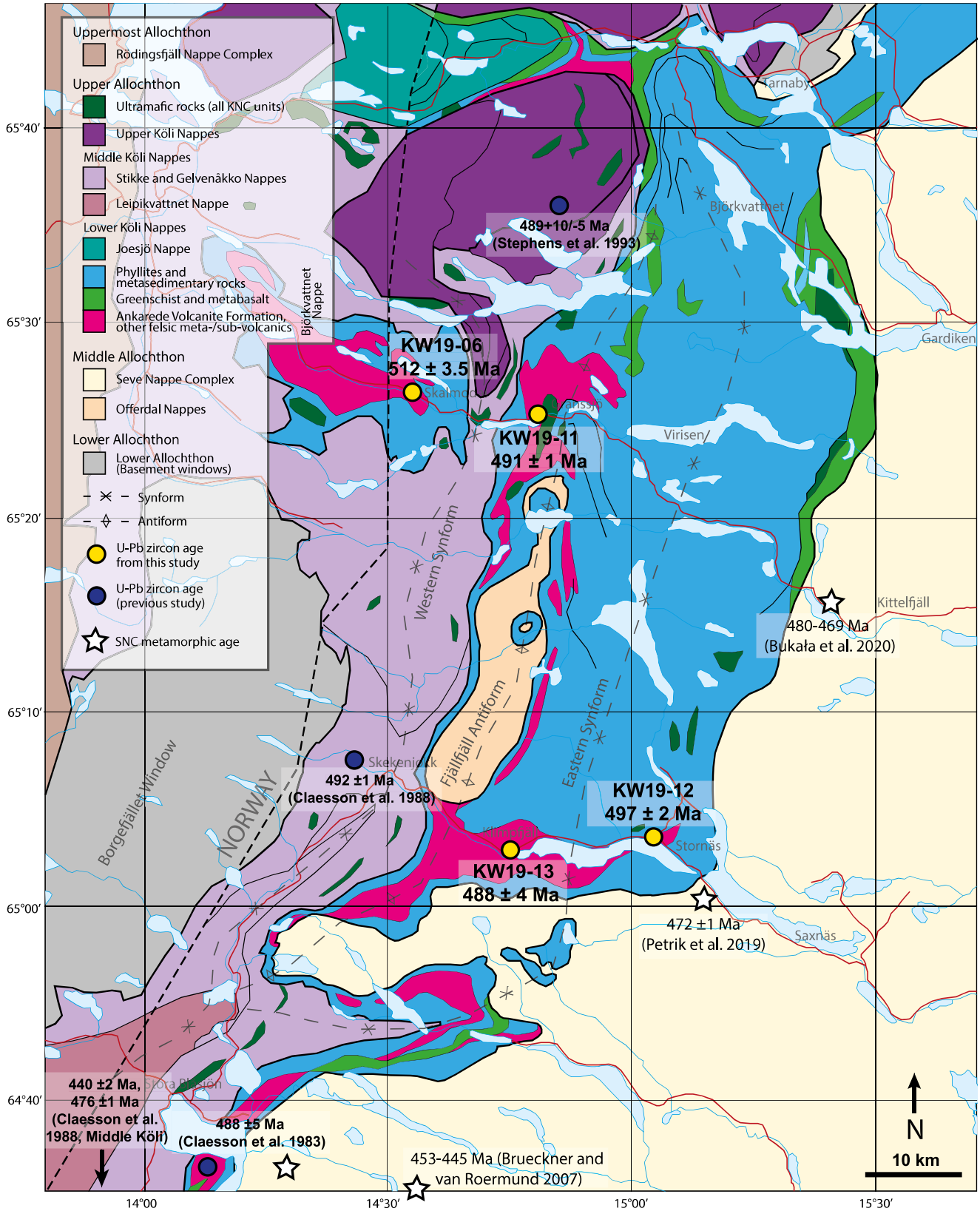

Fig. 2 Simplified map of northwestern Jämtland and southwestern Västerbotten, showing locations of samples. SNC, Seve Nappe Complex. Source: geological map based on SGU map series Ai, numbers 41, 42 (Zachrisson and Sjostrand 1990), 73, 74 (Zachrisson 1991), 75, 76 (Zachrisson 1993), 160, 161, 162 and 163 (Stephens 2001*a*, *b*, *c*, *d*).

hydrothermal alteration and is also metamorphosed at greenschist to lower amphibolite facies conditions (Sjöstrand 1978). Interlayers of phyllitic rocks and tuffites are commonly present in these metavolcanic units. Some coarser-grained varieties of igneous rocks may represent sub-volcanic complexes (Claesson *et al.* 1988). A sub-volcanic intrusion in the AVF at Stora Blåsjön in the south of the study area (Fig. 2) was previously dated at 488 ± 5 Ma (zircon U–Pb; Claesson *et al.* 1983) (Fig. 4).

The AVF has been correlated with the felsic and mafic tuffites in the Gilliks Formation in the eastern limb of the Eastern Synform

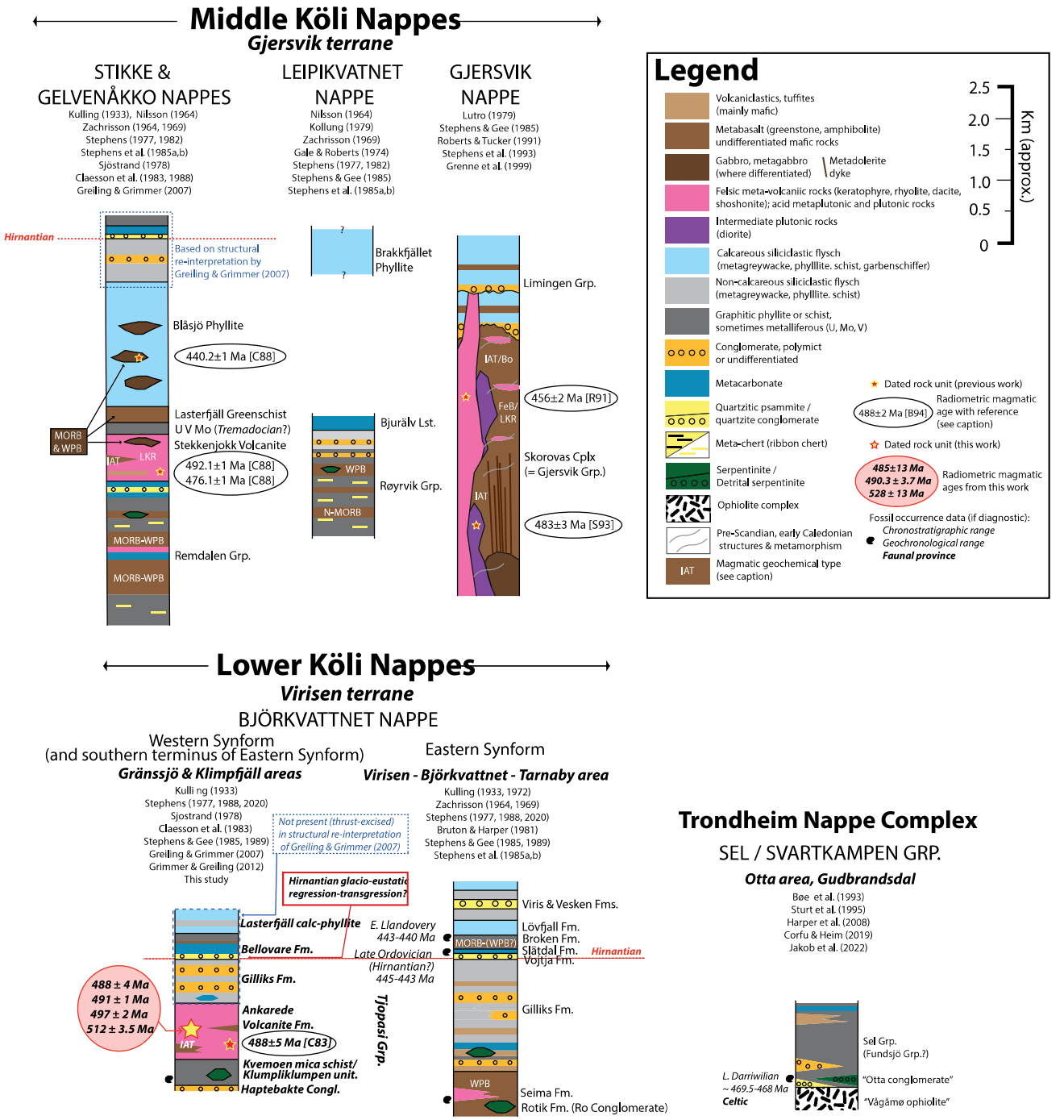

Fig. 3. Lithostratigraphic columns for the Köli and Trondheim nappe complexes organized by lithotectonic unit (nappe) and geographical area, with radiometric ages for magmatic crystallization, geochemical affinities of magmatic rocks, detrital zircon U–Pb age spectra, and fossil occurrences, biostratigraphic ages and faunal provincialism. The set of units in blue boxes are interpreted by Stephens (1982) as belonging to the Lower Köli Nappes and by Greiling and Grimmer (2007) as belonging to the Middle Köli Nappes. Magmatic geochemical discrimination is as in the original publications, mainly based upon the approaches of Pearce and Cann (1973) and Wood (1980); these methods have, however, now been largely updated. MORB, mid-ocean ridge basalt; N-MORB, normal MORB; FeB, ferrobasalt; IAT, island-arc tholeiite; WPB, within-plate basalt; Bo, boninite; Sh, shoshonitic; LKR, low-K rhyolite.

(Stephens and Gee 1985), or is laterally equivalent to the Seima Formation (Stephens 2020). Above the AVF in equivalents to the Gilliks Formation, quartzites, quartzite conglomerates with altered ultramafic clasts, graphitic phyllites, bioclastic carbonates and then quartz-rich turbiditic greywackes occur (Zachrisson 1969), having a bulk trace element pattern suggestive of derivation from a continental magmatic arc (Greiling and Grimmer 2007), either an active Ordovician continental margin or, because the age of the source rocks is unknown, the Fennoscandian craton.

The upper part of the Björkvattnet Nappe in the Eastern Synform, above the Gilliks Formation, comprises quartzite with conglomerate (Vojtja Formation); limestone (Slätdal Formation); and graphitic phyllite with a small amount of tholeiitic pillow basalt (Broken Formation). A diverse shelly fauna in the Slätdal Formation is probably Hirnantian (445–443 Ma) in age (Spjeldnaes 1985). Early Llandovery (*c.* 440 Ma) graptolites are found in the overlying Broken Formation (Kulling 1933). A thick, coarsening-upwards flysch-like succession of calcareous turbiditic greywackes (Lövfjall,

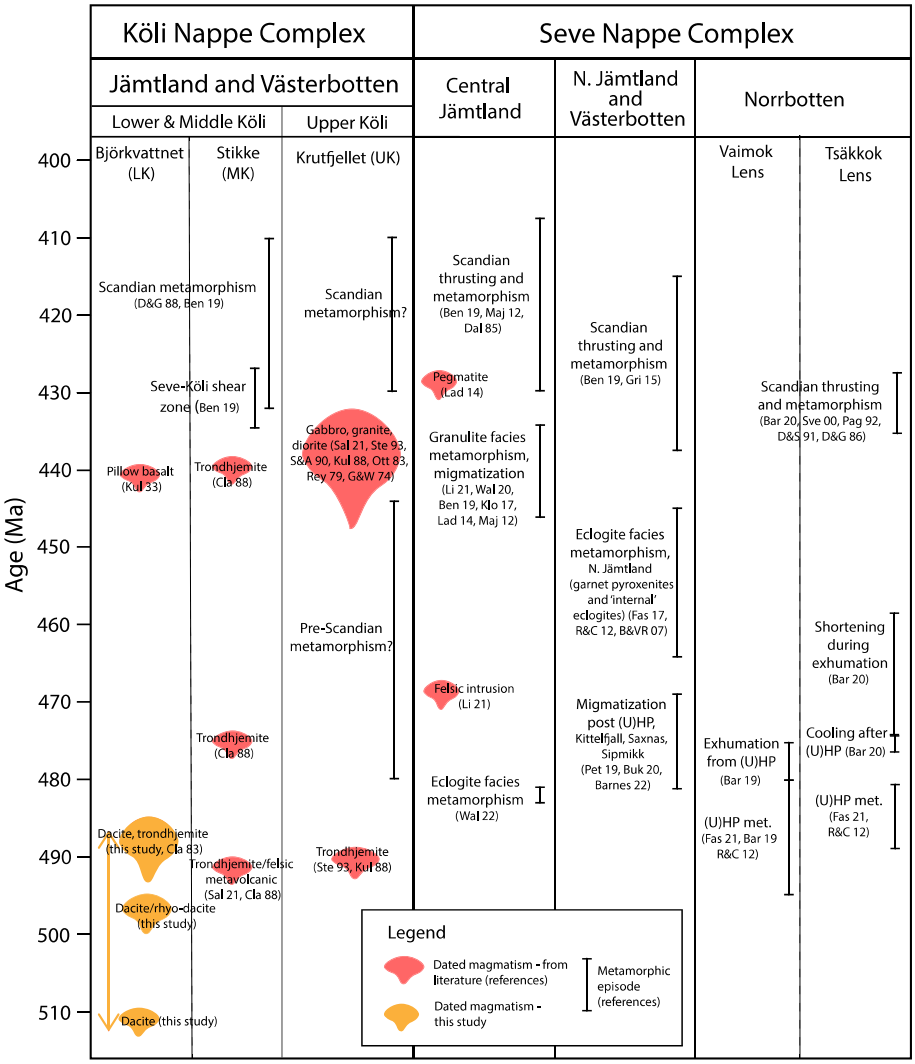

Fig. 4. A summary diagram for all dated episodes of magmatism and metamorphism within the Köli Nappe Complex (KNC) and Seve Nappe Complex (SNC), between 510 and 400 Ma. Source for data: **KNC** – Gee and Wilson (1974); Kullerud *et al.* (1988); Otten (1983); Reymer (1979); Roberts and Tucker (1991); Bender *et al.* (2019); Stephens (2020 and references therein (table 22.2); Saalmann *et al.* (2021); this study. **SNC** – Bender *et al.* (2019); Walczak *et al.* (2022*b*); Barnes *et al.* (2019, 2020, 2022); Bukała *et al.* (2020); Petrík *et al.* (2019); Fassmer *et al.* (2021); Gee *et al.* (2020 and references therein table 21.1).

Vesken and Viris formations) overlies the Broken Formation, and they are the youngest strata in the Björkvattnet Nappe.

The Björkvattnet Nappe has no basement of either continental or ophiolitic character. No internal unconformities have been recognized, hence the stratigraphic succession appears to be continuous. The nappe is affected by two penetrative, foliation-forming deformation phases, D_1 and D_2 (Stephens 1977; Sjöstrand 1978). Metamorphism at greenschist to lower amphibolite facies initiated between D_1 and D_2 and persisted through D_2. Metamorphic rocks with magmatic protoliths have been affected by all deformation and metamorphic phases and have not been seen to cut earlier fabrics (Stephens 1977; Sjöstrand 1978). Given that the youngest rocks are Early Silurian (Kulling 1933; Spjeldnaes 1985), this gives a maximum age for the deformation and metamorphism. Isotopic ages for metamorphic mineral phases range from 433 to 419 Ma (Dallmeyer and Gee 1988; Bender *et al.* 2019) (Fig. 4). The upright, large-scale folding during D_3 deformed both foliations and thrusts, and post-dated peak metamorphism.

Middle and Upper Köli Nappes

The MKN also contain a volcano-sedimentary succession spanning the Late Cambrian and all the Ordovician. In the type area in northern Jämtland and southern Västerbotten and westward into central Norway the Middle Köli Nappes include, in ascending tectonostratigraphic order, the Stikke, Gelvenåkko, Leipikvattnet and Gjersvik nappes (Stephens *et al.* 1985*b*). As in the LKN, the stratigraphically lowest strata (Remdalen Group in the Stikke and Gelvenåkko Nappes and Røyrvik Group in the Leipvikvatnet Nappe, Fig. 3) are metapelites with mafic metavolcanic rocks, including pillow lavas and hyaloclastites, but also including limestone and porphyry (Zachrisson 1969; Stephens 1982). Ultramafic lenses are present in the Remdalen Group but are smaller and less abundant than in the underlying Björkvattnet Nappe.

In the Stikke and Gelvenåkko Nappes, stratigraphically above the Remdalen Group and its equivalents, is an extensive suite of mainly felsic metavolcanic rocks including the Stekenjokk metavolcanic ('Quartz-Keratophyre') unit (Zachrisson 1969; Stephens 1982) composed of felsic pyroclastics and hypabyssal intrusions with subordinate more mafic lavas and intrusions, often altered by sodium metasomatism to quartz keratophyre and spilite. The least altered rocks allow identification of basalt, basaltic andesite, dacite and rhyodacite (Stephens 1982) so the range of compositions resembles that in the AVF of the Björkvattnet Nappe. Sub-volcanic meta-trondhjemites in the Stekenjokk metavolcanic unit have yielded concordant, U–Pb multigrain zircon ages of 492 ± 1 and 476 ± 1 Ma (Claesson *et al.* 1988) (Fig. 4). The overlying sedimentary succession in both the Stikke and Gelvenåkko Nappes (Fig. 3) commences with metalliferous (U, V, Mo) graphitic phyllite and mafic metavolcanic rocks (Lästerfjäll Greenschist). These are succeeded by a thick package of calcareous turbiditic phyllites (Bläsjo Phyllite and the equivalent Brakkfjället Phyllite in the Leipikvattnet Nappe) with hypabyssal mafic and subordinate felsic intrusive sheets including a meta-trondhjemite dated at *c.* 440 Ma (Claesson *et al.* 1988) (Fig. 4). Deformation and greenschist to lower amphibolite facies metamorphism followed a similar evolution to the Björkvattnet Nappe. In the stratigraphically

younger parts of the Stikke and Gelvenåkko Nappes the main foliation and metamorphism post-dates the *c.* 440 Ma metagabbros and trondhjemite in the Blasjö Phyllite and is Silurian in age (Scandian).

These lower nappes are succeeded structurally upwards by the Gjersvik Nappe (Lutro 1979). Its lowest stratigraphic element is a suite of Furongian (or older) island-arc volcanic rocks and plutons (Skorovas Formation. – Halls *et al.* 1977) containing an Early or Middle Ordovician metamorphic fabric, succeeded unconformably by calcareous and volcaniclastic greywackes and phyllites (Limingen Group). These are cut by a suite of 459–456 Ma calc-alkaline plutons consistent with an active continental margin location (Roberts and Tucker 1991; Meyer *et al.* 2003). The Gjersvik Nappe is roofed by the Helgeland Nappe Complex of the Uppermost Allochthon, a Laurentian continental margin assemblage, probably emplaced upon the Gjersvik Nappe before the early Late Ordovician plutonism (Stephens and Gee 1985; Meyer *et al.* 2003).

The Middle Köli Gjersvik nappe wedges out northwards and in its place between the Uppermost Allochthon and the Stikke Nappe appear the Upper Köli Nappes (UKN) (Fig. 1). The Krutfjellet Nappe forms a major tectonostratigraphic component in the UKN, being dominated by turbiditic metasedimentary rocks including a metamorphosed conglomerate containing trondhjemite pebbles with a concordant U–Pb multigrain zircon age of 492 ± 1 as well as mafic, immature arc-like, metavolcanic rocks (Stephens *et al.* 1993; Stephens 2020) (Fig. 4). These rocks show a distinctly higher metamorphic grade than the underlying Köli Nappes. The Krutfjellet Nappe displays an Ordovician regional tectonic foliation which is cut by latest Ordovician to Early Silurian mafic and felsic plutons, demonstrating a pre-Scandian tectonic event followed by an episode of post-arc lithospheric extension (Stephens *et al.* 1993; Saalmann *et al.* 2021). Underlying the Krutfjellet Nappe is the Atofjället Nappe, containing Furongian felsic metavolcanic rocks metamorphosed under amphibolite facies conditions and also with a pre-Scandian metamorphic foliation (Stephens 2020; Saalmann *et al.* 2021).

The Köli Nappes within the terrane concept and the 'Virisen terrane'

Comparison between the Köli Nappes

In the Stikke, Gelvenåkko and Leipikvatnet Nappes, the Cambrian to Early Ordovician parts of their successions (Remdalen and Røyrvik Groups) resemble the lowest stratigraphic elements of the Björkvattnet Nappe (Seima Formation and lower Tjopasi Group; Fig. 3). The succeeding island-arc tholeiite and felsic rocks of the Stekenjokk Quartz Keratophyre are similar in petrology and age to the AVF of the Björkvattnet Nappe but also resemble the Skorovas Formation of the Gjersvik Nappe Fig. and metavolcanic rocks in the Atofjället Nappe (UKN) (Lutro 1979; Claesson *et al.* 1983, 1988; Stephens *et al.* 1985*a*, *b*; Grimmer and Greiling 2012; this work). Boninitic lavas are associated with island-arc tholeiites in the Skorovas Formation which appear to be absent in the lower tectonic elements of the KNC. The Skorovas Formation volcanic rocks are, in turn, broadly co-eval with island-arc volcanic rocks (Fundsjø Group) in the Meråker Nappe (Eastern TNC) (Grenne and Lagerblad 1985; Bjerkgård and Bjørlykke 1994), considered to be at an equivalent tectonostratigraphic level to the Gjersvik Nappe (Stephens and Gee 1985). Hence, with the exception of boninites, there is remarkable consistency in the character and timing of Furongian–Tremadocian volcanism in all these nappes.

At higher stratigraphic levels, depositional and magmatic environments in the different nappes diverge. The metamorphosed calc-turbidites with hypabyssal gabbro sheets in the Stikke, Gelvenåkko and Leipikvatnet Nappes contrast with the quartz-rich, non-calcareous flysch of the Björkvattnet Nappe and its apparent lack of post-arc intrusions. This suggests that the post-arc flysch basins in these two nappe complexes occupied different climate zones or had different source region palaeogeology during the Middle to Late Ordovician (Stephens and Gee 1985; Gee *et al.* 2014; Stephens 2020). By the earliest Silurian, the Stikke and Gelvenåkko Nappes experienced lithospheric extension as indicated by the intrusions, as also found in the Meråker Nappe, while similar intrusions are not present in the Björkvattnet. Nappe. The Gjersvik Nappe has an additional magmatic element in the form of early Late Ordovician mature-arc batholiths which, uniquely in the MKN, form a link to Laurentian crust (Helgeland Nappe Complex, Uppermost Allochthon); their tectonic juxtaposition may have been Middle Ordovician or even earlier (Lutro 1979; Meyer *et al.* 2003), again emphasizing the probable remoteness of the calcareous, post-arc flysch basin fill from Baltica. Grenne *et al.* (1999) also correlated the Gjersvik Nappe (Skorovas Formation) to the Løkken–Hølonda sequence, which has a Laurentian affinity.

There are also contrasts in metamorphic and structural evolution. The Björkvattnet, Stikke and Gelvenåkko Nappes show no evidence for any metamorphism or foliation-forming events prior to the Scandian episode. However, in the Gjersvik and Meråker Nappes (Skorovas Formation and Fundsjø Group) and the Atofjallet and Krutfjellet Nappes, an early foliation in metavolcanic and metasedimentary rocks is cut by the Late Ordovician to Early Silurian intrusions. Furthermore, a Laurentian influence in magmatism, sedimentation and tectonometamorphism becomes more evident when passing to higher levels in the Köli nappe pile, such as early deformation in the Gjersvik Nappe attributed to emplacement on to Laurentian crust (Lutro 1979; Meyer *et al.* 2003).

The Köli Nappes as tectonostratigraphic terranes

Stephens and Gee (1985, 1989) erected a terrane scheme for the Scandinavian Caledonides. Within the KNC, four distinct terranes were recognized, named the Virisen, Gjersvik, Hølonda and 'metamorphic complexes'. The Virisen terrane was uniquely equated with the LKN, exemplified by the Björkvattnet Nappe, the subject of this study (Fig. 2). The Gjersvik terrane comprised the MKN (Stikke, Gelvenåkko, Leipvikvatnet and Gjersvik Nappes) and the Meråker Nappe in the TNC (Fig. 1). The Hølonda terrane was equated with the Støren Nappe situated west of the Gula Nappe, also in the TNC. The 'metamorphic complexes' encompassed the higher-grade Krutfjellet Nappe, but its largest element was the Gula Complex (Nappe) in the axial part of the TNC. Differentiation of the Virisen and Gjersvik terranes was based upon the differing characteristics of their Ordovician, flysch-dominated successions and intrusions as outlined in the previous section. The Virisen terrane became equated to the so-called 'Virisen Arc' in later studies (Dallmeyer and Gee 1986; Brueckner and van Roermund 2004), which was implicated in the collision with the SNC.

The histories and spatial relationships of the terranes have been interpreted in different ways. Stephens and Gee (1985, 1989) regarded the Virisen terrane as an ensimatic arc outboard of Baltica. Their Gjersvik terrane was combined with their 'metamorphic complexes' into a model in which they formed an ensimatic arc that was accreted to Laurentia and combined with the Hølonda terrane to form the foundations of a peri-Laurentian ensialic arc. Grimmer and Greiling (2012) took a different approach, combining the LKN and MKN into different parts of the same extensive ensimatic rifted arc complex, with the LKN in the forearc position. This has some appeal in the light of the key similarities between the earlier elements of the LKN and MKN outlined above, especially the pre-arc and coeval ensimatic arc volcanites, some of which are the subject of this study.

The post-arc history evidently involved development of contrasting basin environments, possibly within a large marginal basin system, and contrasting metamorphic evolution as these basins

impinged at different times upon approaching Laurentian or peri-Laurentian crust. This later evolution of the Furongian–Tremadocian arc edifice gave the distinctive characteristics of the individual Köli Nappes that form the basis of the terrane scheme.

(Ultra-)high-pressure metamorphism within the Seve Nappe Complex

The discovery of eclogite facies rocks in the SNC, especially those recording ultrahigh-pressures, requires a mechanism for the subduction of a large mass of continental margin crust. Collision with an island-arc is a likely solution (Dallmeyer and Gee 1986; Stephens 1988; Brueckner and van Roermund 2004; Majka *et al.* 2014*a*) In this section and in Figure 4, we summarize the occurrences and ages of (U)HP metamorphism in the SNC for comparison with the age span for magmatism in the KNC (see also Gee *et al.* 2020).

The northernmost occurrences of (U)HP metamorphic rocks within the SNC crop out in Norrbotten. The Vaimok lens records peak (U)HP metamorphism at *c.* 495–480 Ma (Root and Corfu 2012; Barnes *et al.* 2019; Fassmer *et al.* 2021) and retrogression after eclogite facies metamorphism (during exhumation) at *c.* 480–475 Ma (Barnes *et al.* 2019) (Fig. 4). The Tsäkkok lens underwent peak (U)HP metamorphism at *c.* 488–482 Ma (Root and Corfu 2012; Fassmer *et al.* 2021) and post-peak cooling at *c.* 477–475 Ma (Barnes *et al.* 2020), with shortening during exhumation continuing until around 458 Ma (Barnes *et al.* 2020) (Fig. 4).

In southern Västerbotten, microdiamond inclusions have been found in the Middle Seve Marsfjället Gneiss near Saxnäs; monazite associated with the microdiamond gave a chemical Th–U–Pb isochron age of 472 ± 3 Ma (Petrík *et al.* 2019), which was originally interpreted as dating UHP metamorphism. However, the age is characterized by dispersion of individual dates between 460 and 479 Ma, so may also contain an age component relating to decompression. Slightly north of this locality in Kittelfjäll, Bukała *et al.* (2020) obtained *c.* 475–469 Ma ages interpreted as dating migmatization under granulite facies conditions related to exhumation from (U)HP (Fig. 4). Also from this locality, monazite cores have been dated to 482 ± 2 Ma (interpreted as onset of a partial melting event), while monazite rims yielded 463 ± 2 Ma interpreted as the onset of cooling and final crystallization of a partial melt (Barnes *et al.* 2022).

UHP metamorphic rocks have also been documented in the Lower Seve Nappes farther south in northern Jämtland at Stor Jougdan (Klonowska *et al.* 2016) and Tjeliken (Majka *et al.* 2014*b*; Fassmer *et al.* 2017). Garnet pyroxenites, garnet peridotites and eclogites from this area have yielded ages of *c.* 465–445 Ma (Bruecker and van Roermund 2007; Root and Corfu 2012; Fassmer *et al.* 2017) (Fig. 4). Solitary orogenic (mantle-derived) ultramafic bodies are very abundant in the SNC. The Friningen body (Middle Seve Nappes) experienced strong deformation at 453–448 Ma (Brueckner and Van Roermund 2007) during a Caledonian prograde metamorphic (subduction) episode that has very similar evolution to the nearby country-rock eclogites and gneisses. Gneisses at Sipmik contain zircons with rims dated to *c.* 483 Ma, interpreted as the timing of an earlier partial melting event (Barnes *et al.* 2022).

In central Jämtland, the Åreskutan Nappe (which forms part of the Middle Seve Nappes) contains migmatitic paragneisses, leucogranites and mafic granulites representing a granulite facies high-T melting event, dated to *c.* 446–435 Ma (Majka *et al.* 2012; Ladenberger *et al.* 2014; Klonowska *et al.* 2017) (Fig. 4). UHP metamorphism, as indicated by evidence such as microdiamond inclusions within garnet is thought to represent an earlier, pre-granulite history (Klonowska *et al.* 2014, 2017, 2021). Evidence for a pre-Silurian anatectic event is also given by an age of 470–468 Ma for a leucogranite inside the Åreskutan Nappe (Li *et al.* 2021). Middle Seve migmatitic paragneisses at Tväråklumparna also contain microdiamond (Majka *et al.* 2014*a*). Zircon U–Pb isotopic depth profiling indicates that (U)HP metamorphism here occurred at or before *c.* 483 Ma, with a later, granulite facies event at around 439 Ma (Walczak *et al.* 2022*b*) (Fig. 4). A leucogranite from the Lower Seve Nappe near Åreskutan has been dated to *c.* 443 Ma (Li *et al.* 2021), likely belonging to the same later granulite facies melting event as in the Middle Seve Nappe (Fig. 4).

A (U)HP metamorphic event at around 490–480 Ma (Fig. 4), has now been identified in all regions of the SNC. In north Jämtland, a second (U)HP metamorphism is also documented, occurring between *c.* 465 and 445 Ma (Fig. 4). In central Jämtland, an episode of granulite facies metamorphism and metamorphism is dated to *c.* 445–435 Ma. Therefore, it is likely that at least the central and southern regions of the SNC have experienced at least two separate (U)HP events.

U–Pb zircon dating and geochemical character of Lower Köli metavolcanic rocks

Methods

Our study area lies in Västerbotten, Sweden, to the south and west of the Björkvattnet–Virisen type area where the lithostratigraphy for the LKN was established (Kulling 1933; Stephens 1977; Fig. 2). Samples of intermediate-felsic metavolcanic rocks were taken from the AVF (LKN) or equivalent units in August 2019. Polished thin-sections were made for petrographic descriptions at AGH University of Science and Technology, Kraków, Poland. Rock samples were crushed and magnetically separated at the Polish Academy of Sciences, Kraków, Poland, and whole-rock major and trace element analyses were performed at Bureau Veritas Commodities Canada, using inductively coupled plasma emission spectrometry (ICP-ES) and inductively coupled plasma mass spectrometry (ICP-MS) on the crushed samples. Separation of zircon was completed at AGH University of Science and Technology using a desktop concentration table and hand separation using a binocular microscope. Separated zircons were mounted in epoxy and then polished to expose the internal parts of the crystals. Cathodoluminescence (CL) and back-scattered electron (BSE) images of mounted grains were obtained using a scanning electron microscope at AGH University of Science and Technology to reveal the internal structure of the zircon and identify analysis spots for dating.

Laser ablation inductively coupled plasma mass spectrometry

U–Pb isotope and trace element analyses of zircon were carried out using laser ablation inductively coupled plasma mass spectrometry (LA-ICP-MS) at the Vegacenter Laboratory, Swedish Museum of Natural History, Stockholm. Uranium and Pb isotope compositions were measured using a Nu Instruments Plasma (II) multi-collector inductively coupled plasma mass spectrometer (MC-ICP-MS) coupled to an ESI NWR193UC excimer laser ablation system. The m/z (mass-to-charge ratio) corresponding to masses ^{202}Pb, ^{204}Pb, ^{206}Pb, ^{207}Pb and ^{208}Pb were measured on ion counters, and those corresponding to ^{232}U, ^{235}U, and ^{238}U were measured on Faraday collectors. The laser was fired for 25 s with a fluence of 1.72 J cm^{-2}, a pulse rate of 7 Hz and a spot size of 20 µm. Helium was used as a sample carrier gas (0.3 l/min) to flush the laser cell and was mixed with argon gas (0.9 l/min) before entering the ICP-MS. All isotope ratios were normalized to the 91 500 zircon reference material with an age of 1065 Ma (Weidenbeck *et al.* 1995). The GJ-1 zircon (609 Ma; Jackson *et al.* 2004; obtained age of 604 ± 12 Ma), Plešovice zircon (337 Ma; Sláma *et al.* 2008; obtained age of 337 ± 8 Ma) and Temora 2 zircon (417 Ma; Black

et al. 2004; obtained age of 420 ± 8 Ma) were utilized as secondary reference materials.

All analytical points have been evaluated based on detailed study of BSE images of all dated zircon grains. BSE imaging was performed after LA-ICP-MS analyses using a JEOL Superprobe 8230 electron microprobe at the Faculty of Geology, Geophysics and Environment Protection, AGH University of Science and Technology (AGH-UST) in Kraków, Poland. The data were processed using the procedure outlined in Kooijman *et al.* (2012). A common Pb correction was applied to a few analyses that had a significant amount of common Pb ($^{206}Pb/^{204}Pb$ lower than 1000) using the model of Stacey and Kramers (1975). Age calculations and construction of concordia diagrams were prepared using the Excel extension Isoplot 3.75 (Ludwig 2012) and the online IsoplotR application (Vermeesch 2018). Trace element analyses were performed with use of AttoM high-resolution ICP-MS coupled to an ESI NWR193UC excimer laser. The laser was fired for 25 s with a fluence of 3 J cm^{-2}, a pulse rate of 8 Hz. The ablation spot diameter was 20 µm. The 91 500 zircon (Wiedenbeck *et al.* 2004) was used as primary reference material. All uncertainties are reported at the 2σ level. Rare-earth element analyses were normalized to CI chondrite values (McDonough and Sun 1995).

Field description and petrography

The samples were all collected from the AVF. They are all of volcanic origin, intermediate to felsic in composition and metamorphosed to greenschist–lower amphibolite facies conditions. Unlike the samples studied by Claesson *et al.* (1983), which were interpreted to have been mainly subvolcanic on the basis of texture, grain size and the local thickening of the formation, our samples are probably all extrusive although their strain state precludes certainty about this. If any of the studied rocks are intrusive, the lack of similar rocks at higher stratigraphic levels constrains their intrusion to being no younger than the obviously extrusive rocks in the same formation, reinforcing their origins as part of the same volcanic edifice as proposed by Claesson *et al.* (1983).

In the following sections, the samples are described from north to south (Fig. 2).

KW19-06

This sample was collected from Skalmodal inside a window of Lower Köli rocks west of and separate from the other samples (Fig. 2). In the area of sampling the exposure is pale with a weak foliation, but is surrounded by rocks that are more phyllitic and darker (Supplementary Fig. S1). There is some compositional and grain-size layering, aligned with the foliation. The rock observed in one thin section is unfoliated and dominated by fine-grained (0.05–0.2 mm) quartz and plagioclase (albite), with minor calcite, chlorite and opaques (mostly pyrite). It contains no porphyroblasts (Supplementary Fig. S2a). A second thin-section is also mostly composed of fine-grained (0.01–0.15 mm) quartz and plagioclase (albite) with minor calcite, white mica and chlorite-biotite. There is also a coarser layer (grain size 0.1–1 mm) that contains a larger proportion of white mica and chlorite–biotite. Porphyroblasts include garnet (Supplementary Fig. S2b), amphibole (Supplementary Fig. S2c) and calcite. Several amphiboles and garnets have experienced partial breakdown to chlorite–biotite. Foliation is formed primarily by micas but some porphyroblasts and quartz lenses are also elongate parallel to the foliation.

KW19-11

This sample was collected from the shore of a small stream near Gränssjö on the eastern limb of the Western Synform (Fig. 2). The exposure was generally pale grey showing a weak foliation (Supplementary Fig. S1). Due to the small size of the exposure, no clear contact with surrounding rocks could be observed. Two thin-sections show a weak foliation formed by alignment of white mica, chlorite and quartz bands. Both samples have a fine-grained (0.05–0.5 mm) matrix composed of plagioclase, quartz and chlorite with minor zoisite, titanite and white mica. In one of the thin-sections, amphiboles 0.2–1 mm in size are common (Supplementary Fig. S2d). Dark, fine-grained, lens-shaped masses, 0.5–1 mm in size are probably relicts of now retrogressed garnet porphyroblasts. In the other thin-section, anhedral titanite is found, mostly concentrated along foliation horizons. Small (0.2–0.4 mm) garnets are occasionally found in tight clusters of up to 10 grains (Supplementary Fig. S2e).

KW19-12

This sample was collected from a quarry at Stornäs in the hinge zone of the Eastern Synform (Fig. 2). It is massive, fine-grained and of pale grey colour. Two thin-sections were studied. In both, the matrix has a moderate grain size (0.2–2 mm) dominated by plagioclase (albite) but also containing quartz, chlorite–biotite, minor titanite and epidote (Supplementary Fig. S2f). Chlorite–biotite and titanite are usually concentrated along cracks or as 'seams' between feldspar and quartz grains. Garnet is not present. There is no foliation.

KW19-13

This sample was collected from a road cut in Klimpfjäll in the hinge zone of the Eastern Synform (Fig. 2). In the exposure the rock is pale greenish-grey with noticeable lamination and foliation (Supplementary Fig. S1). One thin-section has a fine-grained (0.1–1 mm) matrix containing plagioclase (albite), quartz, white mica and chlorite–biotite with minor titanite and epidote (Supplementary Fig. S2g) and contains a single amphibole porphyroblast. There is a weak foliation, defined by aligned chlorite–biotite and white mica. Several cracks are partially infilled by chlorite–biotite and/or calcite. Large crystals (0.5–1.5 mm) of calcite are mostly concentrated in one layer, but there are several other clusters of calcite crystals throughout the thin-section, likely formed due to late fluid infiltration.

A second thin-section has a moderate grain size (0.5–1.5 mm). The majority of the sample has a matrix of white mica, plagioclase (albite), quartz and chlorite–biotite with minor calcite and opaques. White mica generally occurs in monomineralic clusters (bundles). Chlorite–biotite is found as large platy sheets of up to 1 mm. There is a patch containing only coarse (up to 1 mm) quartz, and a band containing >50% calcite. Subhedral to euhedral garnet phenocrysts are common, 0.3–1.5 mm in diameter (Supplementary Fig. S2h). There is a general alignment of white micas within the bundles, but no general overall foliation.

Geochemistry

Based on the Winchester and Floyd (1977) classification using trace elements, sample KW19-11 is andesitic to andesitic/basaltic (based on two samples), KW19-13 is andesitic and KW19-12 is dacitic/rhyodacitic (Fig. 5a). No geochemical data are available for KW19-06. However, it appears to be similar to the other samples and, for this reason, is considered to lie within the same compositional range. These rocks are likely to have experienced metasomatism during hydrothermal alteration (Stephens *et al.* 1985*a*), which may have increased Na and Si contents, therefore alkali–silica plots are not considered an accurate representation of original volcanic composition. On the plot of Th/Yb v. Nb/Yb (Fig. 5b; Pearce 2014), all samples plot within the oceanic arc field, with samples KW19-12 and KW19-13 also overlapping with the edge of the continental arc field.

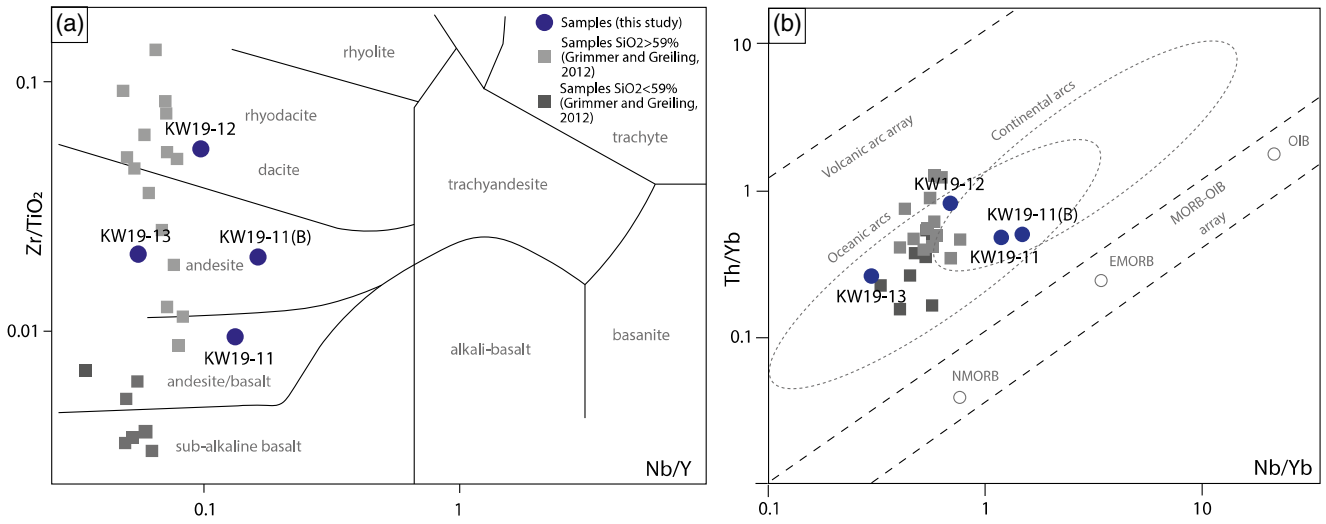

Fig. 5. (**a**) Winchester and Floyd (1977) classification diagram. Grey squares indicate Lower Köli metavolcanic compositions from Grimmer and Greiling (2012). (**b**) Plot of Th/Yb v. Nb/Yb (Pearce 2014).

U–Pb zircon dating results

KW19-06

The sample has zircon grains 50–150 µm in size. The majority of grains are euhedral prismatic crystals. In cathodoluminescence (CL) images, most grains display oscillatory zoning, and occasional sector or irregular zoning (Fig. 6). A couple of grains appear to have distinctive cores, displaying darker CL but also oscillatory zoning.

Analytical spots were placed both in the cores and near the rims. A total of 42 U–Pb analyses were made (Fig. 7a). Twelve of them display strong discordance or even reverse discordance (more than 5% discordance). The remaining $^{206}Pb/^{238}U$ ages spread from 535 ± 8 Ma to 478 ± 7 Ma (Supplementary Table S3). However, during detailed studies of BSE zircon (Supplementary Fig. S4) we found that the youngest date of *c.* 478 Ma was obtained from an analytical point placed in an altered zircon characterized by wavy zoning, thus this date was not considered for further calculations. The oldest date of 535 ± 8 Ma is distinctly older than the other dates obtained for the sample, thus we believe it may be inherited from an earlier history of the rock. Some 26 of the 28 remaining analyses gave a concordia age of 512 ± 4 Ma (Fig. 7b). Two distinctly younger $^{206}Pb/^{238}U$ ages of 484 ± 7 Ma and 493 ± 7 Ma (Supplementary Table S3) were not included in concordia calculations. We believe that they may be at least partially reset as they strongly stand out from the remainder of the group.

Th/U ratios (see Supplementary Table S3) range from 0.50 to 0.92, and Eu anomalies ($Eu/Eu^* = Eu/\sqrt{(Sm*Gd)}$) range from 0.21 to 0.25 (Supplementary Table S5).

KW19-11

Zircon grains are 100–300 µm in size, mostly euhedral prismatic crystals, though the majority are fractured. Most of the grains display oscillatory zoning in CL images (Fig. 6). Some grains appear to have slightly darker cores highlighted by very thin and bright bands. Most of the cores also display oscillatory zoning. Detailed study of BSE images (Supplementary Fig. S4) reveals that most of these grains contain altered (possibly metamict) rims or zones.

A total of 63 points for U–Pb isotopic analyses were placed in cores and mantles (inside and outside of the bright bands) (Fig. 7c). Seven analyses show high U content (more than 900 ppm) and these analyses were not included into further calculations due to possible irradiation damage. The concordant $^{206}Pb/^{238}U$ ages ($n = 47$) are spread out between 520 ± 5 to 476 ± 5 Ma (Fig. 7d; Supplementary Table S3) and no mean age calculations seem reasonable. However, when dates were differentiated into core and mantle locations, we were able to calculate a concordia age for core analyses ($n = 14$), which is 491 ± 3 Ma (Fig. 7e). The core analyses appear to be less affected by altering/metamictization than the mantles, and therefore are less likely to have been partially reset. The remaining mantle analyses still extend from the oldest to youngest obtained dates, so we cannot see any statistical or empirical reason to differentiate them further.

Th/U ratios range from 0.46 to 1.31 for cores and are similar to those of mantles (0.37–0.93). Eu anomalies range from 0.08 to 0.18 for cores and from 0.11 to 0.26 for mantles (Supplementary Table S5).

KW19-12

Zircons range from 50 to 150 µm. Approximately a quarter of grains are euhedral prismatic crystals displaying sector zoning in CL images (Fig. 6). The rest are mostly irregular with irregularly shaped, homogeneous dark CL cores, obviously metamict. They are surrounded by thin, higher CL rims that sometimes display oscillatory zoning.

A total of 40 U–Pb analyses were placed both in cores and rims (Fig. 7f). However, detailed inspection of the position of analytical points in relation to zircon BSE images (Supplementary Fig. S4) revealed that only 21 U–Pb analyses were placed in the sector zoned zircon or in the clear rim (with no mixing with the core) and are less than 5% discordant. Out of this set, 10 analyses show high U content, exceeding 900 ppm, thus they have not been considered for further calculations. The rest of the analyses ($n = 11$) provide $^{206}Pb/^{238}U$ ages bracketing between 506 ± 4 and 479 ± 7 Ma (Supplementary Table S3). Eight out of 11 analyses gave a concordia age of 497 ± 2 Ma (Fig. 7g). However, it is possible that all zircons from the sample have suffered some Pb loss due to metamictization, as most of the dated zircons have a considerably high U content (exceeding 610 ppm). Thus, we emphasize the importance that the age obtained for this sample be considered with care.

Th/U ratios range from 0.29 to 0.86 and Eu anomalies range from 0.29 to 0.86 (Supplementary Table S5), which reflects the large dispersion of trace element concentrations in these zircons. This may be a result of (partial) metamictization.

KW19-13

Zircon grains are generally euhedral, prismatic crystals with lengths between 50 and 150 µm. In CL images most grains display

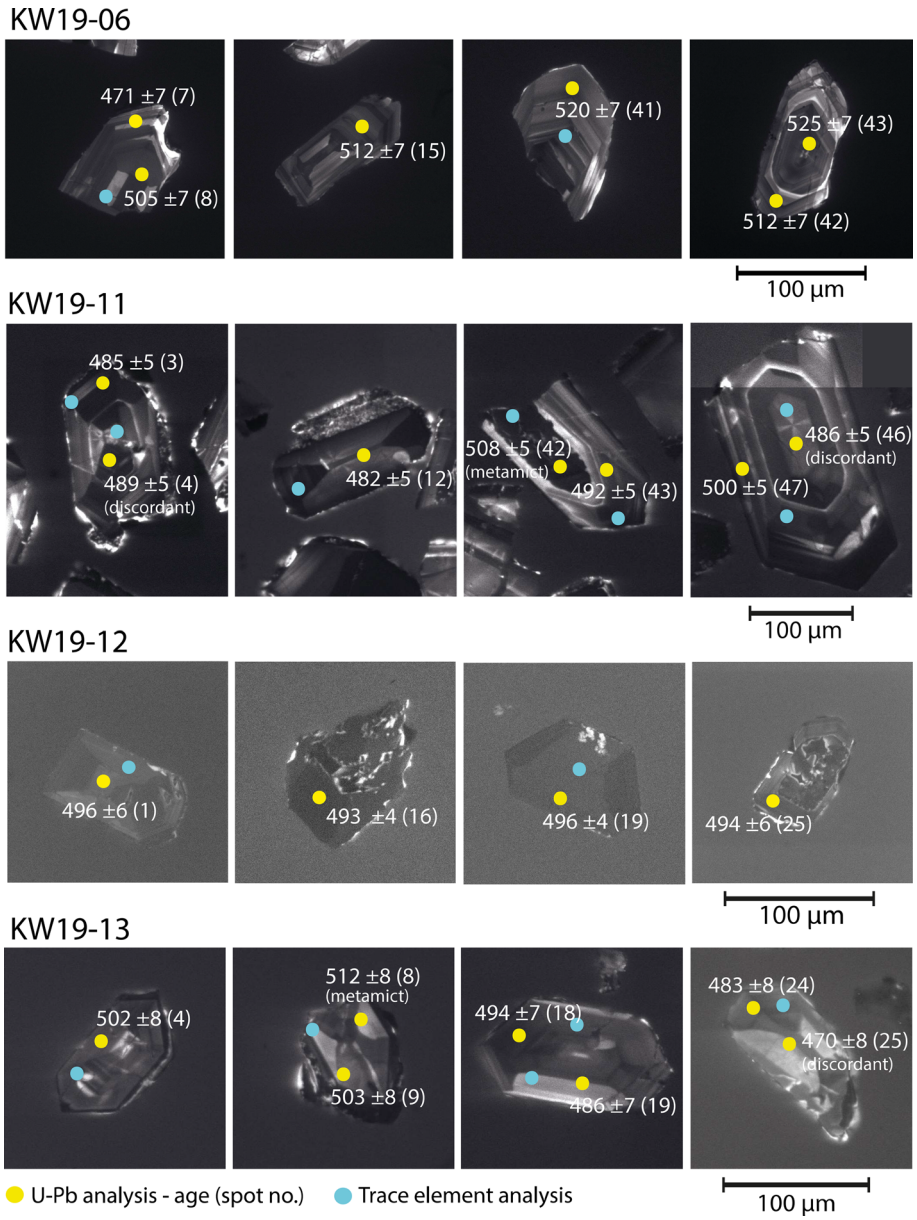

Fig. 6. Representative cathodoluminescence images of analysed zircon grains, showing examples of variation in morphologies. Yellow spots indicate U–Pb analysis points, blue spots indicate trace element analysis points. Ages are $^{206}Pb/^{238}U \pm$ propagated 2σ, with spot number in brackets. Marked U–Pb spots without ages were discordant.

oscillatory zoning, while some are densely fractured and display no obvious zoning (Fig. 6).

A total of 42 U–Pb isotopic analyses have been made (Fig. 7h). Most were discordant by more than 5%. Close inspection of BSE (Supplementary Fig. S4) and CL images reveals that the grains are metamict. This leaves 15 reliable $^{206}Pb/^{238}U$ ages between 524 ± 8 and 473 ± 7 Ma for further consideration (Supplementary Table S3). Of these, the 524 ± 8 Ma is distinctly older. The remaining 14 analyses gave a concordia age of 488 ± 4 Ma (Fig. 7i). Some distinctly younger dates may result from (partial) resetting. Eliminating the two youngest dates, the remaining 12 analyses give a similar concordia age of 491 ± 3 Ma. Discordant age points do not yield any geologically useful information due to large errors. Th/U ratios range from 0.29 to 0.77 and Eu anomalies lie in a tight range from 0.15 to 0.34 with one higher outlier of 0.57 (Supplementary Table S5).

Discussion

The significance of the U–Pb zircon ages from the Björkvattnet Nappe

Our results provide direct ages for AVF felsic metavolcanic to subvolcanic rocks in the Björkvattnet Nappe of the LKN and mostly fit within the span of the older magmatic episode in the KNC (*c.* 492–475 Ma) recognized in previous studies. These also provide a chronological framework for future metamorphic studies. Trace element bulk geochemistry shows a predominantly oceanic arc signature for all samples, consistent with other data for the AVF (Grimmer and Greiling 2012).

The ages of 491 ± 1 Ma (KW19-11, cores) and 488 ± 4 Ma (KW19-13) overlap within error, while the age of 497 ± 2 Ma from sample KW19-12 is slightly older. However, this age must be treated with a degree of caution due to the high U content of the zircons in this sample, which suggests that this sample may have experienced metamictization, so this age is likely to be a minimum age for the sample.

The two youngest ages (KW19-11, KW19-13) in our new dataset broadly agree with previous U–Pb zircon ages found for trondhjemite in the LKN in this region (Fig. 4; Claesson *et al.* 1983). As mentioned above, coeval felsic magmatism has been also dated in the MKN and UKN in the Jämtland/Västerbotten area (Claesson *et al.* 1988; Stephens *et al.* 1993; Saalmann *et al.* 2021). All the aforementioned rocks have the geochemical characteristics of an island-arc setting (e.g. Stephens 1982; Grimmer and Greiling 2012). The 497 ± 2 Ma age of KW19-12 is older than any dated volcanic activity in the KNC.

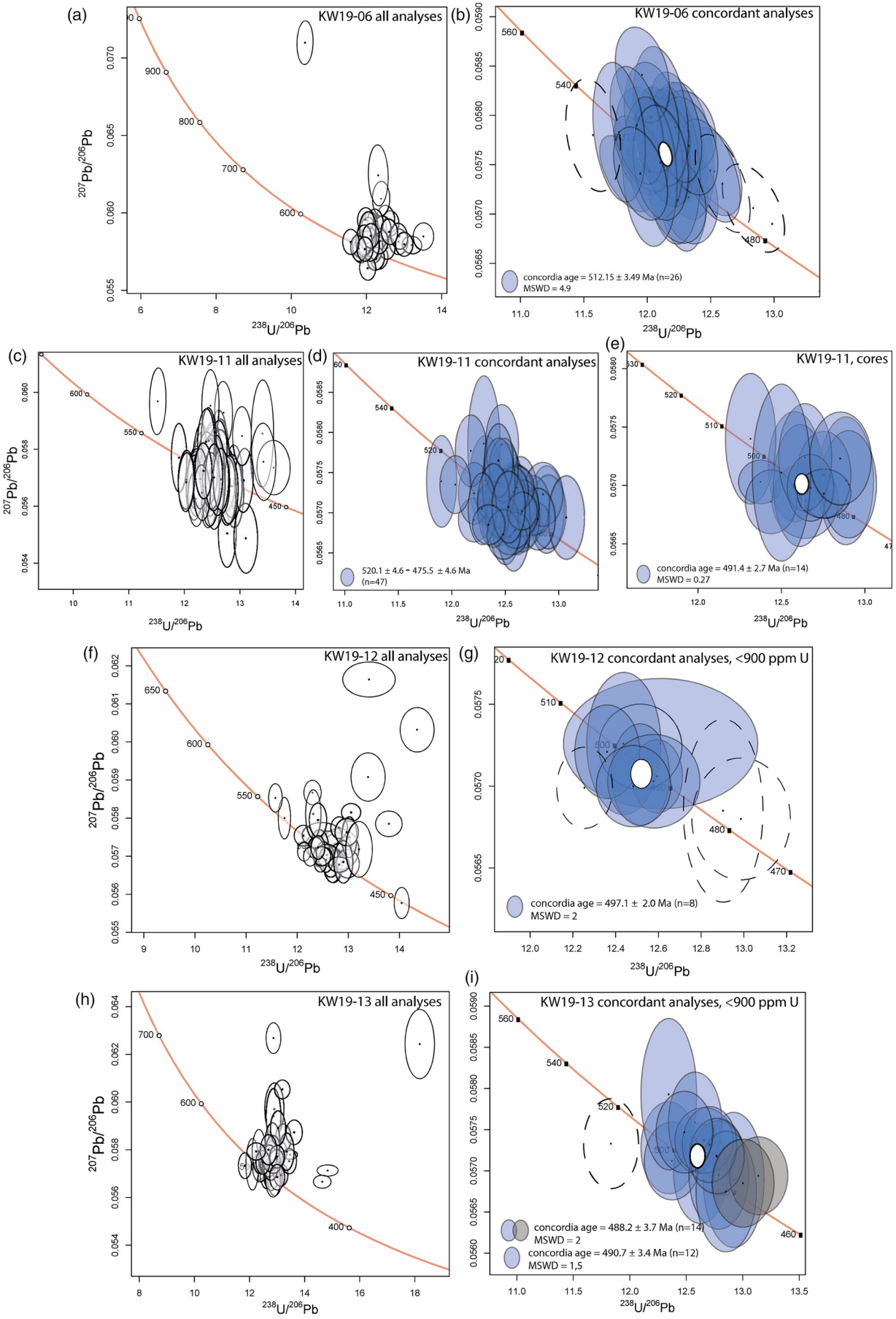

Fig. 7. Concordia diagrams of zircon U–Pb analyses. Both unfiltered (showing all analyses, both concordant and discordant analyses) and filtered (showing only concordant analyses) plots are given.

The age of 512 ± 4 Ma from sample KW19-06 is markedly older than the other samples. The location of this sample is within a window of the LKN, not continuously mappable at outcrop with the units from which the other samples were acquired. The single oldest date of 535 ± 8 Ma, obtained from sample KW19-06, is distinctly older than other dates found within this sample, it is also within error of a single older date of 524 ± 8 Ma found in sample KW19-13. These older dates may represent a component of reworked older (magmatic) zircon. However, it is not possible to make any further deductions based on these individual age points. There is no clear difference between core and rim ages; most cores are clearly magmatic. All the sampled grains in KW19-06 display a consistent trace element pattern (Supplementary Fig. S6) indicating that they formed in the same magmatic-tectonic environment. This sample also yields two significantly younger ages of 484 ± 7 Ma and 493 ± 7 Ma. While these do lie within the range yielded by the other samples, we prefer to attribute a mechanism of (partial) resetting for these two, younger age-points in KW19-06.

The 512 ± 4 Ma age (KW19-06) is older than ages documented in previous studies in the Köli and correlative nappe complexes and coeval only with the ages obtained in the Rödingsfjället Nappe Complex of the Uppermost Allochthon (Slagstad *et al.* 2021). In the Uppermost Allochthon, the arc-related 501 ± 3 Ma metavolcanic rocks of the Moefjellet Group overthrust other arc-related metavolcanic rocks of the Plura Nappe (510 ± 6 Ma) and syntectonic pegmatites (515 ± 5 Ma), and even older metatonalites (541 ± 6 Ma) that intruded a correlative of the Kjerringfjell Group (Slagstad *et al.* 2021). Further field and geochemical studies will be required to constrain the geotectonic affinity of the felsic metavolcanic rock sample with age 512 ± 3.5 Ma. However, our new age data presented here, and data from the Uppermost Allochthon (Slagstad *et al.* 2021) offer the possibility that the subduction history of Iapetus commenced at a time when the Iapetus ocean basin was still relatively young (Waldron *et al.* 2014).

U–Pb zircon ages in relation to biostratigraphic constraints from the Otta conglomerate

The AVF lies above the serpentine conglomerates of the lowest Tjopasi Group and the Seima Formation (Fig. 3). The serpentine conglomerates have been correlated on lithological grounds with detrital serpentinites at Otta in the TNC (Figs 1, 3), where they occur together with fossils dated to Llanvirn (broadly equivalent to the Darriwilian *c.* 467–458 Ma) by Bruton and Harper (1981). This is *younger* than the zircon ages obtained in this study from the overlying AVF. This anomaly prompts us to re-evaluate this correlation.

The monomict Otta serpentine conglomerate forms part of an assemblage of fanglomerates that also contain units with clasts of metabasalt, trondhjemite, psammite, calc-silicate, mica-schist, gneiss, granite and pegmatite, hence the serpentine conglomerate is part of a rudite assemblage that is often polymict and a mix of both oceanic and terrigenous clast types (Bøe *et al.* 1993). Sturt *et al.* (1991) placed the Otta Conglomerate in their Sel Group (Fig. 3) and attempted to show that this lay unconformably on an ophiolite substrate ('Vågåmo Ophiolite'). This was also argued by Bøe *et al.* (1993) who provided better-documented examples of an unconformity. In contrast, the Rotik Formation in the Björkvattnet Nappe (Fig. 3) comprises monomict serpentinite conglomerates and separate but spatially associated, almost monomict, quartzite conglomerates with a few ultramafic clasts (DuRietz 1935). While they are terrigenous, the quartzite conglomerates are highly mature and lack the schist, granitoid and greenstone clasts of the Otta conglomerates. There is no evidence in the Björkvattnet Nappe for an ophiolitic pediment.

The tectonostratigraphic status of the Otta conglomerate has also been controversial. Corfu and Heim (2019), following Strand (1964), included these rocks in the Svartkampen Complex, a unit which can be traced around the Gudbrandsdalen antiform to join the Fundsjø Group, a part of the Meråker Nappe (Sturt *et al.* 1995). The Meråker Nappe records a pre-Scandian deformation and metamorphic history absent from the Björkvattnet Nappe.

These differences between the serpentine conglomerate-bearing units in the Björkvattnet Nappe and at Otta cast doubt upon unifying them into a single metaperidotite-bearing unit (e.g. Jakob *et al.* 2022). The U–Pb zircon ages of the Ankarede metavolcanic rocks show that the underlying serpentinite conglomerates in the Björkvattnet Nappe must be earliest Ordovician or older, at the older end of the biostratigraphic age range suggested by Holmqvist (1980). If, as argued above, the Otta conglomerate is part of the Meråker Nappe, which is often correlated with the Gjersvik Nappe in the MKN (Stephens and Gee 1985), it lies tectonostratigraphically above the detrital serpentinites in the Björkvattnet Nappe.

Correlations between magmatic and metamorphic events in the KNC and SNC

The KNC, in particular the 'Virisen terrane' incorporating the LKN, has been suggested to be the island-arc that collided with the SNC and led to its (U)HP metamorphism (Dallmeyer and Gee 1986; Stephens 1988; Brueckner and van Roermund 2004). The early magmatism (*c.* 512–475 Ma) in the LKN is found to have occurred at a similar time or just prior to the earlier phase of (U)HP metamorphism within the SNC (*c.* 495–480 Ma) (Barnes *et al.* 2019, 2022; Bukała *et al.* 2020; Fassmer *et al.* 2021; Walczak *et al.* 2022*b*) (Fig. 4). This timing makes it possible that the LKN represents the arc that collided with the SNC and leading to (U)HP metamorphism. However, if this is the case, there must only have been a short amount of time between formation of the arc and subduction of the leading edge of Baltica (the SNC). This further suggests that at least part of the Virisen Arc must have been active close to Baltica as there would not have been sufficient time for the arc to move a long distance before collision.

It is also notable that (U)HP metamorphic rocks within the SNC, especially those giving older (U)HP ages of *c.* 488–480 Ma, lie in close proximity to the outcrop of the LKN. The southernmost locations of the Early Ordovician or older (U)HP metamorphism in the SNC (Walczak *et al.* 2022*b*) correlate well with southernmost outcrops of the LKN (Fig. 1). To the north, the Vaimok and Tsäkkok Nappes are the north-extreme outcrops of (U)HP metamorphism in the SNC, with HP metamorphism extending only to the Mårma terrane (Callegari *et al.* 2023). This again corresponds spatially with the northernmost outcrops of the LKN. This is consistent with the Virisen terrane representing the arc that the SNC subducted underneath in the Late Cambrian to Early Ordovician. There is currently no more evidence of subduction of the SNC during this time interval to the south or to the north (Walczak *et al.* 2022*a*).

The stratigraphic succession in the Björkvattnet Nappe extends up to at least the Llandovery (Fig. 3) so has the potential to record sediment sources until well after the collision events experienced by the SNC and inboard Baltica. Stratigraphic and detrital zircon provenance arguments have suggested proximity between the Jämtlandian Nappes (Lower Allochthon) and the LKN, possibly from the Early Ordovician (Gee *et al.* 2014; Stephens 2020). Apart from Gee *et al.* (2014), modern detrital provenance studies of the KNC metasedimentary rocks are lacking but are, arguably, essential to establishing (or refuting) linkages between the KNC, the SNC and the Fennoscandian craton. Geochemical signatures in the Late Ordovician intrusive suite may also help to establish linkages between the KNC and continental substrates on to which they became emplaced.

Conclusions

U–Pb isotope dating of zircon grains from metamorphosed dacitic to andesitic volcanic rocks in the LKN shows magmatic ages of 512 ± 3.5 Ma, 497 ± 2 Ma, 491 ± 1 Ma and 488 ± 4 Ma, constraining the age of magmatism within a volcanic arc system in this allochthon. The three younger ages of 497–488 Ma agree with previous ages found for Lower and Middle Köli volcanic rocks. The oldest age of *c.* 512 Ma is older than previous ages found in the KNC. The timing of volcanism in the LKN adds another line of evidence that refutes a correlation between serpentine conglomerates in the LKN and the Otta conglomerates in the TNC, as those in the LKN are older than those in the TNC. Additionally, the spatial link between the Virisen terrane and rock occurrences of the Late Cambrian to Early Ordovician (U)HP metamorphism of the SNC is noted here. Comparison between ages of magmatism within the KNC and ages of (U)HP metamorphism within the SNC allows for the Virisen terrane to have been the colliding arc that led to subduction of the leading edge of Baltica. At least part of the arc system must have been close to Baltica at an early stage, which is supported by similarity of the Ordovician rock sequences of both.

Scientific editing by Deta Gasser

Acknowledgements We thank Deta Gasser, Michael Stephens, and Fernando Corfu for their helpful comments and reviews. We acknowledge NordSIMS-Vegacenter for provisioning of facilities and experimental support and we would like to thank Melanie Kielman-Schmitt for assistance. This is Vegacenter publication #067.

Author contributions **ISMC**: formal analysis (equal), investigation (lead), writing – original draft (equal), writing – review & editing (lead); **SJC**: conceptualization (equal), writing – original draft (equal), writing – review & editing (supporting); **KW**: formal analysis (equal), investigation (supporting), writing – original draft (supporting), writing – review & editing (supporting); **GZ**: investigation (supporting), writing – review & editing (supporting); **EK**: resources (supporting), writing – review & editing (supporting); **JM**: conceptualization (supporting), writing – review & editing (supporting)

Funding The work was supported by the National Science Centre of Poland, grants no. 2021/41/N/ST10/04298 and no. 2021/41/B/ST10/03679. NordSIMS-Vegacenter is funded by the Swedish Research Council as a national research infrastructure (Dnr. 2021-00276).

Competing interests The authors declare that they have no known competing financial interests or personal relationships that could have appeared to influence the work reported in this paper.

Data availability All data generated or analysed during this study are included in this published article (and its supplementary information files).

References

Andréasson, P.-G. and Albrecht, L.G. 1995. Derivation of 500 Ma eclogites from the passive margin of Baltica and a note on the tectonometamorphic heterogeneity of eclogite-bearing crust. *Geological Magazine*, **132**, 729–738, https://doi.org/10.1017/S001675680001894X

Andréasson, P.G., Gee, D.G. and Suko, S. 1985. Seve eclogites in the Norrbotten Caledonides, Sweden. *In:* Gee, D.G. and Sturt, B.A. (eds) *The Caledonide Orogen – Scandinavia and Related Areas*. Wiley, Chichester, 887–902.

Barnes, C.J., Majka, J. *et al.* 2019. High-spatial resolution dating of monazite and zircon reveals the timing of subduction–exhumation of the Vaimok Lens in the Seve Nappe Complex (Scandinavian Caledonides). *Contributions to Mineralogy and Petrology*, **174**, https://doi.org/10.1007/s00410-018-1539-1

Barnes, C.J., Jeanneret, P., Kullerud, K., Majka, J., Schneider, D.A., Bukała, M. and Klonowska, I. 2020. Exhumation of the high-pressure Tsäkkok Lens, Swedish Caledonides: insights from the structural and white mica $^{40}Ar/^{39}Ar$ geochronological record. *Tectonics*, **39**, https://doi.org/10.1029/2020TC006242

Barnes, C.J., Bukała, M., Callegari, R., Walczak, K., Kooijman, E., Kielman, M. and Jarosław, S. 2022. Zircon and monazite reveal late Cambrian / early Ordovician partial melting of the Central Seve Nappe Complex, Scandinavian Caledonides. *Contributions to Mineralogy and Petrology*, **177**, 92(2022), https://doi.org/10.1007/s00410-022-01958-x

Bender, H., Glodny, J. and Ring, U. 2019. Absolute timing of Caledonian orogenic wedge assembly, Central Sweden, constrained by Rb–Sr multi-mineral isochron data. *Lithos*, **344–345**, 339–359, https://doi.org/10.1016/j.lithos.2019.06.033

Bjerkgård, T. and Bjørlykke, A. 1994. Geology of the Folldal area, southern Trondheim Region Caledonides, Norway. *Norges Geologiske Undersøkelse Bulletin*, **426**, 53–75.

Black, L.P., Kamo, S.L. *et al.* 2004. Improved $^{206}Pb/^{238}U$ microprobe geochronology by the monitoring of a trace-element-related matrix effect; SHRIMP, ID-TIMS, ELA-ICP-MS and oxygen isotope documentation for a series of zircon standards. *Chemical Geology*, **205**, 115–140, https://doi.org/10.1016/j.chemgeo.2004.01.003

Bøe, R., Sturt, B.A. and Ramsay, D.M. 1993. The conglomerates of the Sel Group, Otta-Vaga area, Central Norway: an example of a terrane-linking succession. *Norges Geologiske Undersokelse Bulletin*, **425**, 1–23.

Brueckner, H.K. 2006. Dunk, dunkless and re-dunk tectonics: a model for metamorphism, lack of metamorphism, and repeated metamorphism of HP/UHP terranes. *International Geology Review*, **48**, 978–995, https://doi.org/10.2747/0020-6814.48.11.978

Brueckner, H.K. and van Roermund, H.L.M. 2004. Dunk tectonics: a multiple subduction/eduction model for the evolution of the Scandinavian Caledonides. *Tectonics*, **23**, https://doi.org/10.1029/2003TC001502

Brueckner, H.K. and Van Roermund, H.L.M. 2007. Concurrent HP metamorphism on both margins of Iapetus: Ordovician ages for eclogites and garnet pyroxenites from the Seve Nappe Complex, Swedish Caledonides. *Journal of the Geological Society, London*, **164**, 117–128, https://doi.org/10.1144/0016-76492005-139

Bruton, D.L. and Harper, D.A.T. 1981. Brachiopods and trilobites of the earl y Ordovician serpentine Otta Conglomerate, south central Norway. *Norsk Geologisk Tidsskrift*, **61**, 153–181.

Bruton, D.L. and Harper, D.A.T. 1988. Arenig–Llandovery stratigraphy and faunas across the Scandinavian Caledonides. *Geological Society, London, Special Publications*, **38**, 247–268, https://doi.org/10.1144/GSL.SP.1988.038.01.15

Bukała, M., Klonowska, I. *et al.* 2018. UHP metamorphism recorded by phengite eclogite from the Caledonides of northern Sweden: P–T path and tectonic implications. *Journal of Metamorphic Geology*, **36**, 547–566, https://doi.org/10.1111/jmg.12306

Bukała, M., Majka, J., Walczak, K., Włodek, A., Schmitt, M. and Zagórska, A. 2020. U–Pb zircon dating of migmatitic paragneisses and garnet amphibolite from the high pressure Seve. *Minerals*, **10**, https://doi.org/10.3390/min10040295

Callegari, R., Kośmińska, K., Barnes, C.J., Barker, A.K., Rousku, S., Nääs, E. and Kooijman, E. 2023. Early Neoproterozoic magmatism and Caledonian metamorphism recorded by the Mårma terrane, Seve Nappe Complex, northern Swedish Caledonides. *Journal of the Geological Society, London*, **180**, https://doi.org/10.1144/jgs2022-092

Cawood, P.A., Strachan, R.A., Pisarevsky, S.A., Gladkochub, D.P. and Murphy, J.B. 2016. Linking collisional and accretionary orogens during Rodinia assembly and breakup: implications for models of supercontinent cycles. *Earth and Planetary Science Letters*, **449**, 118–126, https://doi.org/10.1016/j.epsl.2016.05.049

Chew, D.M. and Strachan, R.A. 2014. The Laurentian Caledonides of Scotland and Ireland. *Geological Society, London, Special Publications*, **390**, 45–91, https://doi.org/10.1144/SP390.16

Claesson, S., Klingspor, I. and Stephens, M.B. 1983. U–Pb and Rb–Sr isotopic data on an Ordovician volcanic-subvolcanic complex from the Tjopasi group, Köli Nappes, Swedish Caledonides. *Gff*, **105**, 9–15, https://doi.org/10.1080/11035898309455285

Claesson, S., Stephens, M.B. and Klingspor, I. 1988. U–Pb zircon dating of felsic intrusions, Middle Köli Nappes, central Scandinavian Caledonides (Sweden). *Norsk Geologisk Tidsskrift*, **68**, 89–97.

Cocks, L.R.M. and Torsvik, T.H. 2005. Baltica from the late Precambrian to mid-Palaeozoic times: the gain and loss of a terrane's identity. *Earth-Science Reviews*, **72**, 39–66, https://doi.org/10.1016/j.earscirev.2005.04.001

Cocks, L.R.M. and Torsvik, T.H. 2021. Ordovician palaeogeography and climate change. *Gondwana Research*, **100**, 53–72, https://doi.org/10.1016/j.gr.2020.09.008

Corfu, F. and Heim, M. 2019. Geochronology of Caledonian metamorphic allochthons in the Otta–Heidal region, South Norway; tectonostratigraphic and palaeogeographical implications. *Journal of the Geological Society, London*, **177**, 66–81, https://doi.org/10.1144/jgs2019-010

Corfu, F., Andersen, T.B. and Gasser, D. 2014. The Scandinavian Caledonides: main features, conceptual advances and critical questions. *Geological Society Special Publication*, **390**, 9–43, https://doi.org/10.1144/SP390.25

Dallmeyer, R.D. and Gee, D.G. 1986. $^{40}r/^{39}Ar$ mineral dates from retrogressed eclogites within the Baltoscandian miogeocline: implications for a polyphase Caledonian orogenic evolution (Sweden). *Geological Society of America Bulletin*, **97**, 26–34, https://doi.org/10.1130/0016-7606(1986)97<26:AMDFRE>2.0.CO;2

Dallmeyer, R.D. and Gee, D.G. 1988. Polyorogenic $^{40}Ar/^{39}Ar$ mineral age record in the Seve and Köli Nappes of the Gäddede area, Northwestern Jämtland, Central Scandinavian Caledonides. *The Journal of Geology*, **96**, 181–198, https://doi.org/10.1086/629208

Domeier, M. 2016. A plate tectonic scenario for the Iapetus and Rheic oceans. *Gondwana Research*, **36**, 275–295, https://doi.org/10.1016/j.gr.2015.08.003

DuRietz, T. 1935. Peridotites, serpentines, and soapstones of northern Sweden, with special reference to some occurrences in Northern Jämtland. *Geologiska Föreningen i Stockholm Förhandlingar*, **57**, 133–260, https://doi.org/10.1080/11035893509445975

Fassmer, K., Klonowska, I. *et al.* 2017. Middle Ordovician subduction of continental crust in the Scandinavian Caledonides: an example from Tjeliken, Seve Nappe Complex, Sweden. *Contributions to Mineralogy and Petrology*, **172**, https://doi.org/10.1007/s00410-017-1420-7

Fassmer, K., Froitzheim, N., Janák, M., Strohmeyer, M., Bukała, M., Lagos, M. and Münker, C. 2021. Diachronous collision in the Seve Nappe Complex: evidence from Lu–Hf geochronology of eclogites (Norrbotten, North Sweden). *Journal of Metamorphic Geology*, **39**, 819–842, https://doi.org/10.1111/jmg.12591

Gale, G.H. and Roberts, D. 1974. Trace element geochemistry of Norwegian Lower Palaeozoic basic volcanics and its tectonic implications. *Earth and Planetary Science Letters*, **22**, 380–390, https://doi.org/10.1016/0012-821X(74)90148-4

Gee, D. 1975. A tectonic model for the central part of the Scandinavian Caledonides. *American Journal of Science*, **275**, 468–515, https://doi.org/10.2475/ajs.277.5.647

Gee, D.G. and Stephens, M.B. 2020. Regional context and tectonostratigraphic framework of the early–middle Paleozoic Caledonide orogen, northwesten Sweden. *Geological Society, London, Memoirs*, **50**, 481–494, https://doi.org/10.1144/m50-2017-21

Gee, D.G. and Wilson, M.R. 1974. The age of orogenic deformation in the Swedish Caledonides. *American Journal of Science*, **274**, 1–9, https://doi.org/10.2475/ajs.274.1.1

Gee, D.G., Kumpulainen, R., Roberts, D., Stephens, M.B., Zachrisson, E. and Thon, A. 1985. *Scandinavian Caledonides – Tectonostratigraphic Map. Scale 1:2 000 000*. Sveriges Geologiska Undersökning, **Ba 35**.

Gee, D.G., Ladenberger, A., Dahlqvist, P., Majka, J., Be'Eri-Shlevin, Y., Frei, D. and Thomsen, T. 2014. The Baltoscandian margin detrital zircon signatures of the central scandes. *Geological Society, London, Special Publications*, **390**, 131–155, https://doi.org/10.1144/SP390.20

Gee, D.G., Klonowska, I., Andréasson, P.G. and Stephens, M.B. 2020. Middle thrust sheets in the Caledonide Orogen, Sweden: the outer margin of Baltica, the continent–ocean transition zone and late Cambrian–Ordovician subduction–accretion. *Geological Society, London, Memoirs*, **50**, 517–548, https://doi.org/10.1144/M50-2018-73

Greiling, R.O. and Grimmer, J.C. 2007. Köli nappes in the north-central Swedish Caledonides – new views on stratigraphy and structural evolution. *Gff*, **129**, 141–153, https://doi.org/10.1080/11035890701292141

Grenne, T. and Lagerblad, B. 1985. The Fundsjo Group, Central Norway – a Lower Palaeozoic island arc sequence: geochemistry and regional implications. *In*: Gee, D.G. and Sturt, B.A. (eds) *The Caledonide Orogen – Scandinavia and Related Areas*. Wiley, Chichester, 745–762.

Grenne, T., Ihlen, P.M. and Vokes, F.M. 1999. Scandinavian Caledonide metallogeny in a plate tectonic perspective. *Mineralium Deposita*, **34**, 422–471, https://doi.org/10.1007/s001260050215

Grimmer, J.C. and Greiling, R.O. 2012. Serpentinites and low-K island arc metavolcanic rocks in the Lower Köli Nappe of the central Scandinavian Caledonides: Late Cambrian–early Ordovician serpentinite mud volcanoes in a forearc basin? *Tectonophysics*, **541–543**, 19–30, https://doi.org/10.1016/j.tecto.2012.03.014

Hacker, B.R., Andersen, T.B., Johnston, S., Kylander-Clark, A.R.C., Peterman, E.M., Walsh, E.O. and Young, D. 2010. High-temperature deformation during continental-margin subduction and exhumation: the ultrahigh-pressure Western Gneiss Region of Norway. *Tectonophysics*, **480**, 149–171, https://doi.org/10.1016/j.tecto.2009.08.012

Häggbom, O. 1978. Polyphase deformation of a discontinuous nappe in the central Scandinavian Caledonides. *Gff*, **100**, 349–354, https://doi.org/10.1080/11035897809454473

Halls, C., Reinsbakken, A., Ferriday, I., Haugen, A. and Rankin, A. 1977. Geological setting of the Skorovas orebody within the allochthonous Gjersvik Nappe, central Norway. *Geological Society, London, Special Publications*, **7**, 128–151, https://doi.org/10.1144/GSL.SP.1977.007.01.16

Harper, D.A.T., Bruton, D.L. and Rasmussen, C.M.O. 2008. The Otta brachiopod and trilobite fauna: palaeogeography of Early Palaeozoic terranes and biotas across Baltoscandia. *Fossils and Strata*, **54**, 31–40, https://doi.org/10.18261/9781405186643-2008-04

Hollocher, K., Robinson, P., Walsh, E. and Roberts, D. 2012. Geochemistry of amphibolite-facies volcanics and gabbros of the Støren nappe in extensions west and southwest of Trondheim, Western Gneiss Region, Norway: a key to correlations and paleotectonic settings. *American Journal of Science*, **312**, 357–416, https://doi.org/10.2475/04.2012.01

Holmqvist, A. 1980. Ordovician gastropods from Vardofjallet, Swedish Lapland, and the dating of Caledonian serpentine conglomerates. *Geologiska Föreningens i Stockholm Förhandlingar*, **102**, 493–487, https://doi.org/10.1080/11035898009454502

Jackson, S.E., Pearson, N.J., Griffin, W.L. and Belousova, E.A. 2004. The application of laser ablation-inductively coupled plasma-mass spectrometry to in situ U–Pb zircon geochronology. *Chemical Geology*, **211**, 47–69, https://doi.org/10.1016/j.chemgeo.2004.06.017

Jakob, J., Andersen, T.B., Mohn, G., Kjøll, H.J. and Beyssac, O. 2022. Revised tectono-stratigraphic scheme for the Scandinavian Caledonides and its implications for our understanding of the Scandian orogeny. *Geological Society of America Special Papers*, **554**, https://doi.org/10.1130/2022.2554(14)

Klonowska, I., Majka, J., Janák, M., Gee, D.G. and Ladenberger, A. 2014. Pressure–temperature evolution of a kyanite-garnet pelitic gneiss from Åreskutan: evidence of ultra-high-pressure metamorphism of the Seve Nappe Complex, west-central Jämtland, Swedish Caledonides. *Geological Society, London, Special Publications*, **390**, 321–336, https://doi.org/10.1144/SP390.7

Klonowska, I., Janák, M., Majka, J., Froitzheim, N. and Kośmińska, K. 2016. Eclogite and garnet pyroxenite from Stor Jougdan, Seve Nappe Complex, Sweden: implications for UHP metamorphism of allochthons in the Scandinavian Caledonides. *Journal of Metamorphic Geology*, **34**, 103–119, https://doi.org/10.1111/jmg.12173

Klonowska, I., Janák, M., Majka, J., Petrík, I., Froitzheim, N., Gee, D.G. and Sasinková, V. 2017. Microdiamond on Åreskutan confirms regional UHP metamorphism in the Seve Nappe Complex of the Scandinavian Caledonides. *Journal of Metamorphic Geology*, **35**, 541–564, https://doi.org/10.1111/jmg.12244

Klonowska, I., Majka, J., Janák, M., Petrík, I., Froitzheim, N., Gee, D.G. and Cuthbert, S. 2021. Comment on the paper: "Evolution of a gneiss in the Seve nappe complex of central Sweden – Hints at an early Caledonian, medium-pressure metamorphism" by Li *et al.* (2020). *Lithos*, **400–401**, 106067, https://doi.org/10.1016/j.lithos.2021.106067

Kollung, S. 1979. Stratigraphy and major structures of the Grong District, Nord Trondelag. *Norges Geologiske Undersøkelse*, **354**, 1–51.

Kooijman, E., Berndt, J. and Mezger, K. 2012. U–Pb dating of zircon by laser ablation ICP-MS: recent improvements and new insights. *European Journal of Mineralogy*, **24**, 5–21, https://doi.org/10.1127/0935-1221/2012/0024-2170

Kullerud, K., Stephens, M.B. and Claesson, S. 1988. Age constraints on exotic arc–basin complexes and tectonic implications, central Scandinavian Caledonides. *Gff*, **110**, 402–403.

Kulling, O. 1933. Bergbyggnaden inom Björkvattnet – Virisen-området i Västerbottensfjällens centrala del. *Geologiska Föreningen i Stockholm Förhandlingar*, **55**, 167–422, https://doi.org/10.1080/11035893309450934

Kulling, O. 1972. The Swedish Caledonides. *In:* de Sitter, L.U., Strand, T. and Kulling, O. (eds) *Scandinavian Caledonides*. Regional Geology Series. John Wiley & Sons, London, 147–285.

Ladenberger, A., Be'eri-Shlevin, Y., Claesson, S., Gee, D.G., Majka, J. and Romanova, I.V. 2014. Tectonometamorphic evolution of the Åreskutan Nappe – Caledonian history revealed by SIMS U–Pb zircon geochronology. *Geological Society, London, Special Publications*, **390**, 337–368, https://doi.org/10.1144/SP390.10

Li, Y., Gee, D.G., Ladenberger, A. and Sjöström, H. 2021. Timing of deformation, metamorphism and leucogranite intrusion in the lower part of the Seve Nappe Complex in central Jämtland, Swedish Caledonides. *GFF*, **143**, 55–70, https://doi.org/10.1080/11035897.2020.1858341

Ludwig, K.R. 2012. *User's Manual for Isoplot Version 3.75–4.15: A Geochronological Toolkit for Microsoft Excel*. Berkley Geochronological Centre, Special Publication, **5**.

Lutro, O. 1979. The geology of the Gjersvik area, Nord-Trondelag, central Norway. *Norges Geologiske Undersøkelse*, **354**, 53–100.

Majka, J., Be'eri-Shlevin, Y., Gee, D.G., Ladenberger, A., Claesson, S., Konečny, P. and Klonowska, I. 2012. Multiple monazite growth in the Åreskutan migmatite: evidence for a polymetamorphic Late Ordovician to Late Silurian evolution in the Seve Nappe Complex of west-central Jämtland, Sweden. *Journal of Geosciences*, **57**, 3–23, https://doi.org/10.3190/jgeosci.112

Majka, J., Rosén, Å *et al.* 2014*a*. Microdiamond discovered in the Seve Nappe (Scandinavian Caledonides) and its exhumation by the 'vacuum-cleaner' mechanism. *Geology*, **42**, 1107–1110, https://doi.org/10.1130/G36108.1

Majka, J., Janák, M., Andersson, B., Klonowska, I., Gee, D.G., Rosén, Å and Kośmińska, K. 2014*b*. Pressure–temperature estimates on the Tjeliken eclogite: new insights into the (ultra)-high-pressure evolution of the Seve Nappe Complex in the Scandinavian Caledonides. *Geological Society, London, Special Publications*, **390**, 369–384, https://doi.org/10.1144/SP390.14

McDonough, W.F. and Sun, S. 1995. The composition of the Earth. *Chemical Geology*, **120**, 223–253, https://doi.org/10.1016/0009-2541(94)00140-4

Meyer, G.B., Grenne, T. and Pedersen, R.B. 2003. Age and tectonic setting of the Nesåa Batholith: implications for Ordovician arc development in the Caledonides of Central Norway. *Geological Magazine*, **140**, 573–594, https://doi.org/10.1017/S0016756803008069

Nilsson, G. 1964. *Berggrunden inom Blåsjöområdet i nordvästra Jämtlandsfjällen*. Sveriges Geologiska Undersökning. Series C, **595**.

Otten, M.T. 1983. *The Magmatic and Subsolidus Evolution of the Artfjället Gabbro, Central Swedish Caledonides*. University of Utrecht.

Page, L.M. 1992. $^{40}Ar/^{39}Ar$ geochronological constraints on timing of deformation and metamorphism of the Central Norrbotten Caledonides, Sweden. *Geological Journal*, **27**, 127–150, https://doi.org/10.1002/gj.3350270204

Pearce, J.A. 2014. Immobile element fingerprinting of ophiolites. *Elements*, **10**, 101–108, https://doi.org/10.2113/gselements.10.2.101

Pearce, J.A. and Cann, J.R. 1973. Tectonic setting of basic volcanic rocks determined using trace element analyses. *Earth and Planetary Science Letters*, **19**, 290–300, https://doi.org/10.1016/0012-821X(73)90129-5

Petrík, I., Janák, M. *et al.* 2019. Monazite behaviour during metamorphic evolution of a diamond-bearing gneiss: a case study from the Seve Nappe

Complex, Scandinavian Caledonides. *Journal of Petrology*, **60**, 1773–1796, https://doi.org/10.1093/petrology/egz051
Pickering, K.T. and Smith, A.G. 1995. Arcs and backarc basins in the Early Paleozoic Iapetus Ocean. *Island Arc*, **4**, 1–67, https://doi.org/10.1111/j.1440-1738.1995.tb00132.x
Reymer, A.P.G. 1979. *Investigations into the Metamorphic Nappes of the Central Scandinavian Caledonides on the Basis of Rb–Sr and K–Ar Age Determinations*. PhD thesis, Bern University.
Robert, B., Domeier, M. and Jakob, J. 2021. On the origins of the Iapetus Ocean. *Earth Science Reviews*, **221**, 103791, https://doi.org/10.1016/j.earscirev.2021.103791
Roberts, D. and Tucker, R.D. 1991. U–Pb zircon age of the Møklevatnet granodiorite, Gjersvik Nappe, *Central Norwegian Caledonides. Norges Geologiske Undersokelse Bulletin*, **421**, 33–38.
Roberts, D., Nordgulen, Ø and Melezhik, V. 2007. The Uppermost Allochthon in the Scandinavian Caledonides: from a Laurentian ancestry through Taconian orogeny to Scandian crustal growth on Baltica. *Geological Society of America Memoirs*, **200**, https://doi.org/10.1130/2007.1200(18)
Root, D. and Corfu, F. 2012. U–Pb geochronology of two discrete Ordovician high-pressure metamorphic events in the Seve Nappe Complex, Scandinavian Caledonides. *Contributions to Mineralogy and Petrology*, **163**, 769–788, https://doi.org/10.1007/s00410-011-0698-0
Saalmann, K., Bjerkgård, T., Slagstad, T., Sandstad, J.S., Lutro, O., Keiding, J.B. and Snook, T.L.A. 2021. Revised tectonostratigraphy and structural evolution of the Köli Nappe Complex, Central Caledonides in Nordland, Norway. *Journal of the Geological Society, London*, **178**, https://doi.org/10.1144/jgs2020-214
Sjöstrand, T. 1978. *Caledonian Geology of the Kvarnbergsvattnet Area, Northern Jämtland, Central Sweden: Stratigraphy, Metamorphism, Deformation*. Sveriges geologiska undersökning, Series C, **735**
Slagstad, T. and Kirkland, C.L. 2018. Timing of collision initiation and location of the Scandian orogenic suture in the Scandinavian Caledonides. *Terra Nova*, **30**, 179–188, https://doi.org/10.1111/ter.12324
Slagstad, T., Saalmann, K. *et al.* 2021. Late Neoproterozoic through Silurian tectonic evolution of the Rödingsfjället Nappe Complex, orogen-scale correlations and implications for the Scandian suture. *Geological Society, London, Special Publications*, **503**, 279–304, https://doi.org/10.1144/SP503-2020-10
Sláma, J., Košler, J. *et al.* 2008. Plešovice zircon – a new natural reference material for U–Pb and Hf isotopic microanalysis. *Chemical Geology*, **249**, 1–35, https://doi.org/10.1016/j.chemgeo.2007.11.005
Spjeldnaes, N. 1985. Upper Ordovician Bryozoans from Ojl Myr, Gotland, Sweden. *Bulletin of the Geological Institutions of the University of Uppsala, N.S.*, **10**, 1–66.
Stacey, J.C. and Kramers, J. 1975. Approximation of terrestrial lead isotope evolution by a two-stage model. *Earth and Planetary Science Letters*, **26**, 207–221, https://doi.org/10.1016/0012-821X(75)90088-6
Stephens, M. 1977. *Stratigraphy and Relationship Between Folding, Metamorphism and Thrusting in the Tärna-Björkvattnet Area, Northern Swedish Caledonides*. Sveriges geologiska undersökning Series C, **726**, https://apps.sgu.se/geolagret/GetMetaDataById?id=md-188b4a19-ace0-42a8 -8abc-98be80a0511a
Stephens, M.B. 1980. Occurrence, nature and tectonic significance of volcanic and high-level intrusive rocks within the Swedish Caledonides. *In:* Wones, D.R. (ed.) *The Caledonides in the U.S.A.* Virginia Polytechnic State University Department Geological Sciences Memoir **2**, 289–298.
Stephens, M.B. 1982. *Field Relationships, Petrochemistry and Petrogenesis of the Stekenjokk Volcanites, Central Swedish Caledonides*. Sveriges Geologiska Undersökning, Series C, **786**.
Stephens, M.B. 1988. The Scandinavian Caledonides: a complexity of collisions. *Geology Today*, **4**, 20–26, https://doi.org/10.1111/j.1365-2451.1988.tb00537.x
Stephens, M.B. 2001*a*. Berggrundskartan 24E Joesjö NO-24F Tärna NV, scala 1:50 000. **Ai 160**.
Stephens, M.B. 2001*b*. Berggrundskartan 24E Joesjö SO-24F Tärna V, scala 1:50 000. **Ai 161**.
Stephens, M.B. 2001*c*. Berggrundskartan 24F Tärna SO, scala 1:50 000. **Ai 162**.
Stephens, M.B. 2001*d*. Berggrundskartan 24F Tärna NO, scala 1:50 000. **Ai 163**.
Stephens, M.B. 2020. Upper and uppermost thrust sheets in the Caledonide orogen, Sweden: outboard oceanic and exotic continental terranes. *Geological Society, London, Memoirs*, **50**, 549–575, https://doi.org/10.1144/m50-2019-12
Stephens, M.B. and Gee, D.G. 1985. A tectonic model for the evolution of the terranes in the central Scandinavian Caledonides. *In:* Gee, D.G. and Sturt, B.A. (eds) *The Caledonide Orogen – Scandinavia and Related Areas*. Wiley, Chichester, 953–978.
Stephens, M.B. and Gee, D.G. 1989. Terranes and polyphase accretionary history in the Scandinavian Caledonides. *Geological Society of America Special Papers*, **230**, 17–30, https://doi.org/10.1130/SPE230-p17
Stephens, M.B. and Van Roermund, H.L.M. 1984. Occurrence of glaucophane and crossite in eclogites of the Seve nappes, southern Norrbotten Caledonides, Sweden. *Norsk Geologisk Tidsskrift*, **64**, 155–163.
Stephens, M.B., Furnes, H., Robins, B. and Sturt, B.A. 1985*a*. Igneous activity within the Scandinavian Caledonides. *In:* Gee, D.G. and Sturt, B.A. (eds) *The Caledonide Orogen – Scandinavia and Related Areas*. Wiley, Chichester, 623–656.
Stephens, M.B., Gustavson, M., Ramberg, I.B. and Zachrisson, E. 1985*b*. The Caledonides of central-north Scandinavia - a tectonostratigraphic overview. *In:* Gee, D.G. and Sturt, B.A. (eds) *The Caledonide Orogen – Scandinavia and Related Areas*. Wiley, Chichester, 135–162.
Stephens, M.B., Kullerud, K. and Claesson, S. 1993. Early Caledonian tectonothermal evolution in outboard terranes, central Scandinavian Caledonides: new constraints from U–Pb zircon dates. *Journal of the Geological Society, London*, **150**, 51–56, https://doi.org/10.1144/gsjgs.150.1.0051
Strand, T. 1964. Otta-dekket og Valdres-gruppen i strøkene langs Bøverdalen og Leirdalen. *Norges Geologiske Undersøkelse Bulletin*, **228**, 280–288.
Sturt, B.A., Ramsay, D.M. and Neuman, R. 1991. The Otta Conglomerate, the Vågåmo Ophiolite – further indications of early Ordovician orogenesis in the Scandinavian Caledonides. *Norsk Geologisk Tidsskrift*, **71**, 107–115.
Sturt, B.A., Boe, R., Ramsay, D.M. and Bjerkgard, T. 1995. Stratigraphy of the Otta-Vaqa tract and regional stratigraphic implications. *Norges Geologisk Undersokelse Bulletin*, **427**, 25–28.
Torsvik, T.H. and Cocks, L.R.M. 2013. Gondwana from top to base in space and time. *Gondwana Research*, **24**, 999–1030, https://doi.org/https://doi.org/10.1016/j.gr.2013.06.012
Van Roermund, H. 1985. Eclogites of the Seve Nappe, central Scandinavian Caledonides. *In:* Gee, D.G. and Sturt, B.A. (eds) *The Caledonide Orogen – Scandinavia and Related Areas*. Wiley, Chichester, 873–886.
Van Staal, C.R. and Dewey, J.F. 2023. A review and tectonic interpretation of the Taconian–Grampian tract between Newfoundland and Scotland: diachronous accretion of an extensive forearc–arc–backarc system to a hyperextended Laurentian margin and subsequent subduction polarity reversal. *Geological Society, London, Special Publications*, **531**, https://doi.org/10.1144/SP531-2022-152
Van Staal, C.R. and Zagorevski, A. 2023. Paleozoic tectonic evolution of the rifted margins of Laurentia. *Geological Society of America Memoirs*, **220**, https://doi.org/10.1130/2022.1220(24)
Vermeesch, P. 2018. IsoplotR: a free and open toolbox for geochronology. *Geoscience Frontiers*, **9**, 1479–1493, https://doi.org/10.1016/j.gsf.2018.04.001
Walczak, K., Ziemniak, G. *et al.* 2022*a*. Late Neoproterozoic extended continental margin development recorded by the Seve Nappe Complex of the northern Scandinavian Caledonides. *Lithos*, **416–417**, https://doi.org/10.1016/j.lithos.2022.106640
Walczak, K., Barnes, C.J., Majka, J., Gee, D.G. and Klonowska, I. 2022*b*. Zircon age depth-profiling sheds light on the early Caledonian evolution of the Seve Nappe Complex in west-central Jämtland. *Geoscience Frontiers*, **13**, https://doi.org/10.1016/j.gsf.2020.11.009
Waldron, J.W.F., Schofield, D.I., Brendan Murphy, J. and Thomas, C.W. 2014. How was the Iapetus Ocean infected with subduction? *Geology*, **42**, 1095–1098, https://doi.org/10.1130/G36194.1
Weidenbeck, M., Alle, P. *et al.* 1995. Three natural standards for U–Th–Pb, Lu–Hf, trace element and REE analyses. *Geostandards Newsletter*, **19**, 1–23, https://doi.org/10.1111/j.1751-908X.1995.tb00147.x
Wiedenbeck, M., Hanchar, J.M. *et al.* 2004. Further characterisation of the 91500 zircon crystal. *Geostandards and Geoanalytical Research*, **28**, 9–39, https://doi.org/10.1111/j.1751-908X.2004.tb01041.x
Winchester, J.A. and Floyd, P.A. 1977. Geochemical discrimination of different magma series and their differentiation products using immobile elements. *Chemical Geology*, **20**, 325–343, https://doi.org/10.1016/0009-2541(77)90057-2
Wood, D.A. 1980. The application of a ThHfTa diagram to problems of tectonomagmatic classification and to establishing the nature of crustal contamination of basaltic lavas of the British Tertiary Volcanic Province. *Earth and Planetary Science Letters*, **50**, 11–30, https://doi.org/10.1016/0012-821X(80)90116-8
Zachrisson, E. 1964. *The Remdalen Syncline*. Sveriges geologiska undersökning, Series C, **596**
Zachrisson, E. 1969. *Caledonian Geology of Northern Jämtland-Southern Västerbotten*. Sveriges Geologiska Undersökning Series C, **644**
Zachrisson, E. 1991. Berggrundskartorna 23E Sipmeke, 1:50 000. **Ai 73-74**.
Zachrisson, E. 1993. Berggrundskartorna 23F Fatmomakke NV och SV, 1:50 000. **Ai 75-76**.
Zachrisson, E. and Sjostrand, T. 1990. Berggrundskartorna (22D-)22E Frostviken, 1:50 000. **Ai 41-42**.